ELECTRONIC SUPPORTING INFORMATION

Highly active iron catalysts for olefin hydrogenation enable *para*hydrogen induced hyperpolarisation of ^{1}H and ^{19}F NMR resonances at 1.4 Tesla

Julianna S. Doll,[a,†] Jan Kergassner,[b,†] Bingyu Zhang,[b] Christina M. Thiele,[c] Gerd Buntkowsky,[b] Markus Enders,[a] Torsten Gutmann,*[b] and Dragos-Adrian Roșca*[a,d]

[a] Anorganisch-Chemisches Institut, Universität Heidelberg, Im Neuenheimer Feld 270, D-69120 Heidelberg, Germany

[b] Technische Universität Darmstadt, Eduard-Zintl-Institut für Anorganische and Physikalische Chemie, Peter-Grünberg-Straße 8, D-64287 Darmstadt, Germany

[c] Technische Universität Darmstadt, Clemens-Schöpf-Institut für Organische Chemie und Biochemie, Peter-Grünberg-Straße 16, D-64287 Darmstadt, Germany

[d] Institut des Sciences Chimiques de Rennes, Université de Rennes, F-35000, Rennes, France

[†] Equal contribution

* Corresponding authors: Torsten Gutmann: gutmann@chemie.tu-darmstadt.de,

Dragos-Adrian Roșca: dragos.rosca@uni-heidelberg.de
dragos-adrian.rosca@univ-rennes.fr

Table of Contents

1 Catalytic hydrogenation

1.1 General remarks

All manipulations were performed in a nitrogen filled MBraun glovebox.

The iron catalysts employed, **1** and **2**, were prepared according to literature procedures.[1]

NMR spectroscopy ^{1}H, $^{13}C\{^{1}H\}$, ^{19}F NMR spectra were recorded using a Bruker Avance II-400 or Bruker Avance III HD 600 MHz spectrometer. The latter was equipped with a Helium cooled, broadband cryoprobe (CP2.1 BBO). Deuterated solvents were distilled from the appropriate drying agents, degassed by three freeze-pump-thaw cycles and stored over 4 Å molecular sieves prior to use. ^{1}H NMR spectra were referenced to the residual protons of the deuterated solvent used. $^{13}C\{^{1}H\}$ NMR spectra were referenced internally to the D-coupled ^{13}C resonances of the NMR solvent. Where appropriate, resonances were assigned using 2D NMR homo- and heterocorrelation (COSY, HMBC, HSQC) techniques. Chemical shifts (δ) are given in ppm, relative to tetramethylsilane (TMS), coupling constants (*J*) in Hz. Unless otherwise stated, resonances are reported at 22 °C.

1.2 General protocol of hydrogenation with Na[(PNN)Fe(N_2)H] and product characterisation data

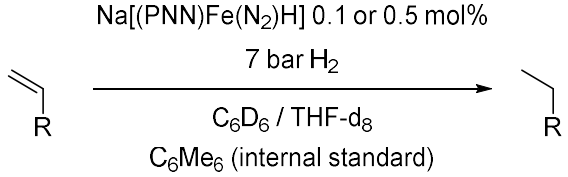

In a thick-walled NMR tube, the corresponding alkene (182.98 µmol, 1.00 equiv.) was dissolved in C_6D_6 (0.34 mL for reactions with 0.1 mol% of catalyst and 0.30 mL for reactions with 0.5 mol% of catalyst). The internal standard, C_6Me_6 was subsequently added (50 µL of a stock solution of 15 mg in 0.5 mL C_6D_6). A solution of **2** in THF-d_8 (18.3 mM, 10 µL for 0.1 mol% catalyst loadings, 50 µL for 0.5 mol% catalyst loadings) was then added to the reaction mixture. A control ^{1}H NMR measurement was performed to ensure no polymerisation took place. Subsequently, the NMR tube was pressurized with 7 bar of hydrogen (99.999 %) and vigorously shaken by hand or on a Fisherbrand™ Nutating Mixer (Variable Speed; 2 rpm). The conversion was determined by NMR spectroscopy with respect to the internal standard.

1-Ethyl-4-fluorobenzene

Following the general procedure, 1-ethenyl-4-fluorobenzene (**3**) (22.35 mg, 21.8 µL, 182.98 µmol) was hydrogenated with 0.1 mol% catalyst. The conversion was complete after 10 min of vigorous shaking.

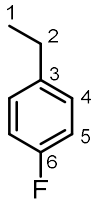

^{1}H NMR (600 MHz, C_6D_6 / THF-d_8, 295 K) δ [ppm] = 6.82 – 6.76 (m, 4H, H4+H5), 2.30 (q, *J* = 7.6 Hz, 2H, H2), 0.98 (t, *J* = 7.6 Hz, 3H, H1).

^{13}C{^{1}H} NMR (151 MHz, C_6D_6 / THF-d_8, 295 K) δ [ppm] = 161.7 (CF, d, *J* = 242.7 Hz, C6), 139.8 (C_q, d, *J* = 3.2 Hz, C3), 129.4 (C_{arom}H, d, *J* = 7.7 Hz, C4), 115.2 (C_{arom}H, d, *J* = 21.0 Hz, C5), 28.2 (CH_2, C2), 15.8 (CH_3, C1).

^{19}F NMR (565 MHz, C_6D_6 / THF-d_8, 295 K) δ [ppm] = −117.97 - −118.02 (m, F6).

The NMR data are in accordance with those previously reported.[2]

Ethylbenzene

Following the general procedure, styrene (**4**) (19.06 mg, 20.9 µL, 182.98 µmol) was hydrogenated with 0.1 mol% catalyst. The conversion was complete after 10 min of vigorous shaking.

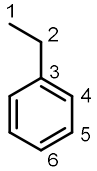

^{1}H NMR (600 MHz, C_6D_6 / THF-d_8, 295 K) δ [ppm] = 7.17 – 7.15 (m, 2H, C_{arom}H), 7.08 – 7.04 (m, 3H, C_{arom}H), 2.44 (q, *J* = 7.6 Hz, 2H, H2), 1.07 (t, *J* = 7.6 Hz, 3H, H1).

^{13}C{^{1}H} NMR (151 MHz, C_6D_6 / THF-d_8, 295 K) δ [ppm] = 144.3 (C_q, C3), 128.6 (C_{arom}H, C5), 128.1 (C_{arom}H, C4), 125.9 (C_{arom}H, C6), 29.2 (CH_2, C2), 15.8 (CH_3, C1).

The NMR data are in accordance with those previously reported.[3]

1-Ethyl-4-methoxybenzene

Following the general procedure, 1-ethenyl-4-methoxybenzene (**5**) (24.55 mg, 24.5 µL, 182.98 µmol) was hydrogenated with 0.1 mol% catalyst. The conversion was complete after 13 min of vigorous shaking.

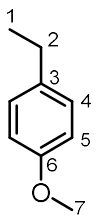

^{1}H NMR (600 MHz, C_6D_6 / THF-d_8, 295 K) δ [ppm] = 6.99 (d, *J* = 8.5 Hz, 2H, H4), 6.80 (d, *J* = 8.5 Hz, 2H, H5), 3.35 (s, 3H, H7), 2.45 (q, *J* = 7.6 Hz, 2H, H2), 1.11 (t, *J* = 7.6 Hz, 3H, H1).

^{13}C{^{1}H} NMR (151 MHz, C_6D_6 / THF-d_8, 295 K) δ [ppm] = 158.4 (C_q, C6), 136.3 (C_q, C3), 129.0 (C_{arom}H, C4), 114.1 (C_{arom}H, C5), 54.7 (CH_3, C7), 28.3 (CH_2, C2), 16.2 (CH_3, C1).

The NMR data are in accordance with those previously reported.[4]

1-Ethyl-2-fluorobenzene

Following the general procedure, 1-ethenyl-2-fluorobenzene (**6**) (22.35 mg, 21.8 µL, 182.98 µmol) was hydrogenated with 0.5 mol% catalyst. The conversion was complete after 3 min of vigorous shaking.

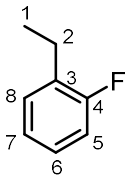

^{1}H NMR (600 MHz, C_6D_6 / THF-d_8, 295 K) δ [ppm] = 6.93 – 6.90 (m, 1H, C_{arom}H), 6.88 – 6.81 (m, 3H, C_{arom}H), 2.51 (q, *J* = 7.6 Hz, 2H, H2), 1.05 (t, *J* = 7.6 Hz, 3H, H1).

^{13}C{^{1}H} NMR (151 MHz, C_6D_6 / THF-d_8, 295 K) δ [ppm] = 161.5 (CF, d, *J* = 244.1 Hz, C4), 131.1 (C_q, d, *J* = 15.9 Hz, C3), 130.1 (C_{arom}H, d, *J* = 5.2 Hz, C8), 127.6 (C_{arom}H, d, *J* = 8.0 Hz, C6/7), 124.2 (C_{arom}H, d, *J* = 3.6 Hz, C6/7), 115.3 (C_{arom}H, d, *J* = 22.2Hz, C5), 22.4 (CH_2, d, *J* = 2.9 Hz, C2), 14.5 (CH_3, d, *J* = 1.0 Hz, C1).

^{19}F NMR (565 MHz, C_6D_6 / THF-d_8, 295 K) δ [ppm] = −119.55 - −119.59 (m, F4).

The NMR data are in accordance with those previously reported.[5]

Ethylcyclohexane

Following the general procedure, vinylcyclohexane (**7**) (20.16 mg, 25.1 µL, 182.98 µmol) was hydrogenated with 0.5 mol% catalyst. The conversion was complete after 3 min of vigorous shaking.

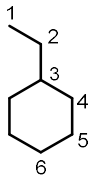

^{1}H NMR (600 MHz, C_6D_6 / THF-d_8, 295 K) δ [ppm] = 1.67 – 1.65 (m, 4H, H4+H5), 1.62 – 1.60 (m, 1H, H6), 1.21 – 1.10 (m, 5H, H2+H5+H6), 1.07 – 1.02 (m, 1H, H3), 0.85 (t, *J* = 7.4 Hz, 3H, H1), 0.82 – 0.78 (m, 2H, H4).

^{13}C{^{1}H} NMR (151 MHz, C_6D_6 / THF-d_8, 295 K) δ [ppm] = 39.8 (CH, C3), 33.3 (CH_2, C4), 30.5 (CH_2, C2), 27.1 (CH_2, C6), 26.8 (CH_2, C5), 11.6 (CH_3, C1).

The NMR data are in accordance with those previously reported.[6]

2,2-Dimethylbutane

Following the general procedure, 3,3-dimethylbut-1-ene (**8**) (15.40 mg, 24.7 µL, 182.98 µmol) was hydrogenated with 0.1 mol% catalyst. The conversion was complete after 40 min of vigorous shaking.

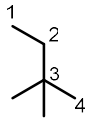

^{1}H NMR (600 MHz, C_6D_6 / THF-d_8, 295 K) δ [ppm] = 1.18 (q, *J* = 7.5 Hz, 2H, H2), 0.85 (s, 9H, H4), 0.80 (t, *J* = 7.5 Hz, 3H, H1).

^{13}C{^{1}H} NMR (151 MHz, C_6D_6 / THF-d_8, 295 K) δ [ppm] = 36.8 (CH_2, C2), 30.5 (C_q, C3), 29.1 (CH_3, C4), 9.2 (CH_3, C1).

The NMR data are in accordance with those previously reported.[3]

Isopropylbenzene

Following the general procedure, 2-phenylpropene (**9**) (21.62 mg, 23.8 µL, 182.98 µmol) was hydrogenated with 0.5 mol% catalyst. The conversion was complete after 17 days of vigorous shaking.

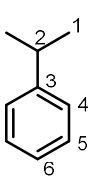

^{1}H NMR (600 MHz, C_6D_6 / THF-d_8, 295 K) δ [ppm] = 7.19 – 7.17 (m, 2H, C_{arom}H), 7.11 – 7.06 (m, 3H, C_{arom}H), 2.71 (sep, *J* = 6.9 Hz, 1H, H2), 1.14 (d, *J* = 6.9 Hz, 6H, H1).

^{13}C{^{1}H} NMR (151 MHz, C_6D_6 / THF-d_8, 295 K) δ [ppm] = 148.9 (C_q, C3), 128.6 (C_{arom}H, C4/5/6), 126.6 (C_{arom}H, C4/5/6), 126.1 (C_{arom}H, C4/5/6), 34.4 (CH, C2), 24.1 (CH_3, C1).

The NMR data are in accordance with those previously reported.[7]

Norbornane

Following the general procedure norbornene (**10**) (17.23 mg, 182.98 µmol) was hydrogenated with 0.5 mol% catalyst. The conversion was complete after 10 min of vigorous shaking.

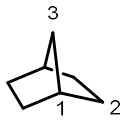

^{1}H NMR (600 MHz, C_6D_6 / THF-d_8, 295 K) δ [ppm] = 2.13 (br s, 2H, H1), 1.42 – 1.41 (m, 4H, H2), 1.13 (br s, 2H, H3), 1.11 – 1.10 (m, 4H, H2).

^{13}C{^{1}H} NMR (151 MHz, C_6D_6 / THF-d_8, 295 K) δ [ppm] =38.6 (CH_2, C3), 36.7 (CH, C1), 30.0 (CH_2, C2).

The NMR data is in accordance with those previously reported.[8]

4-Ethylcyclohexene and ethylcyclohexane

Following the general procedure, vinylcyclohexene (**11**) (19.80 mg, 23.9 µL, 182.98 µmol) was hydrogenated with 0.1 mol% catalyst. The reaction was completed after 15 min of vigorous shaking to give 4-ehylcyclohexene.

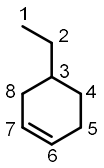

^{1}H NMR (600 MHz, C_6D_6 / THF-d_8, 295 K) δ [ppm] = 5.66 (br s, 2H, H6+H7), 2.02 – 1.99 (m, 1H, H8), 1.96 – 1.95 (m, 2H, H5), 1.63 – 1.61 (m, 1H, H4), 1.58 – 1.54 (m, 1H, H8), 1.38 – 1.31 (m, 1H, H3), 1.24- 1.17 (m, 2H, H2), 1.15 – 1.10 (m, 1H, H4), 0.82 (t, *J* = 7.4 Hz, 3H, H1).

^{13}C{^{1}H} NMR (151 MHz, C_6D_6 / THF-d_8, 295 K) δ [ppm] = 127.1 (CH, C6/C7), 126.9 (CH, C6/C7), 35.6 (CH, C3), 31.9 (CH_2, C8), 29.7 (CH_2, C2), 28.9 (CH_2, C4), 25.6 (CH_2, C5), 11.5 (CH_3, C1).

The NMR data are in accordance with those previously reported.[9]

The internal double bound was not hydrogenated when using 0.1 mol% of catalyst. With 0.5 mol% catalyst, full hydrogenation was observed after 118 h shaking on the nutating mixer, to obtain ethylcyclohexane.

(*E*)-But-1-en-1-ylbenzene and *n*-butylbenzene

Following the general procedure, (*E*)-buta-1,3-dien-1-ylbenzene (**12**) (23.82 mg, 25.6 µL, 182.98 µmol) was hydrogenated with 0.5 mol% catalyst. The conversion was complete after 30 min of vigorous shaking.

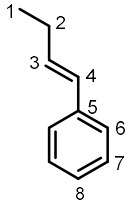

^{1}H NMR (600 MHz, C_6D_6 / THF-d_8, 295 K) δ [ppm] = 7.27 – 7.26 (m, 2H, H6), 7.17 – 7.14 (m, 2H, H7, overlapping with C_6D_6), 7.07 – 7.04 (m, 1H, H8), 6.31 (d, *J* = 15.8 Hz, 1H, H4), 6.13 (dt, *J* = 15.8; 6.6 Hz, 1H, H3), 2.05 (q, *J* = 7.2 Hz, 2H, H2), 0.96 (t, *J* = 7.5 Hz, 3H, H1).

^{13}C{^{1}H} NMR (151 MHz, C_6D_6 / THF-d_8, 295 K) δ [ppm] = 138.3 (C_q, C5), 132.2 (CH, C3), 129.5 (CH, C4), 128.7 (C_{arom}H, C7), 127.0 (C_{arom}H, C8), 126.3 (C_{arom}H, C6), 26.3 (CH_2, C2), 13.8 (CH_3, C1).

The NMR data are in accordance with those previously reported.[10]

The further hydrogenation of the internal double bond could be performed in the presence of 0.5 mol% catalyst after 83.5 h while shaking on the nutating mixer.

***n*-Butylbenzene**

Following the general procedure, but-3-en-1-ylbenzene (**13**) (24.19 mg, 27.5 µL, 182.98 µmol) was hydrogenated with 0.1 mol% catalyst. No more starting material was observed after 15 min of vigorous shaking. In addition to hydrogenation, isomerization to 1-phenyl-2-butene (18 %, E/Z ratio 3.8:1) and (*E*)-1-phenyl-1-butene (11 %) was observed. Full hydrogenation to *n*-butylbenzene was observed after 83.5 h.

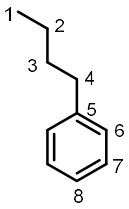

^{1}H NMR (600 MHz, C_6D_6 / THF-d_8, 295 K) δ [ppm] = 7.19 – 7.15 (m, 2H, H6/7), 7.09 – 7.06 (m, 3H, H6/7+H8), 2.47 (t, *J* = 7.7 Hz, 2H, H4), 1.51 – 1.46 (m, 2H, H3), 1.26 – 1.20 (m, 2H, H2), 0.84 (t, *J* = 7.3 Hz, 3H, H1).

^{13}C{^{1}H} NMR (151 MHz, C_6D_6 / THF-d_8, 295 K) δ [ppm] = 142.9 (C_q, C5), 128.7 ($C_{arom}H$, C6), 128.5 ($C_{arom}H$, C7), 125.9 ($C_{arom}H$, C8), 36.0 (CH_2, C4), 34.0 (CH_2, C3), 22.6 (CH_2, C2), 14.1 (CH_3, C1).

The NMR data are in accordance with those previously reported.[2]

Hexane

Following the general procedure, 1-hexene (**14**) (15.40 mg, 23.0 µL, 182.98 µmol) was hydrogenated with 0.1 mol% catalyst. No more starting material was observed after 5 min of vigorous shaking. In addition to hydrogenation, isomerization to 2-hexene (26.6 %, E/Z ratio 3.5:1) and 3-hexene (5.7 %) was observed.

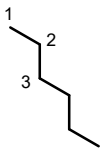

^{1}H NMR (600 MHz, C_6D_6 / THF-d_8, 295 K) δ [ppm] = 1.28 – 1.21 (m, 8H, H2+H3), 0.89 (t, *J* = 7.1 Hz, 6H, H1).

^{13}C{^{1}H} NMR (151 MHz, C_6D_6 / THF-d_8, 295 K) δ [ppm] = 31.9 (CH_2, C3), 23.0 (CH_2, C2), 14.3 (CH_3, C1).

The NMR data are in accordance with those previously reported.[11]

1.3 NMR spectra of hydrogenation products

1-Ethyl-4-fluorobenzene

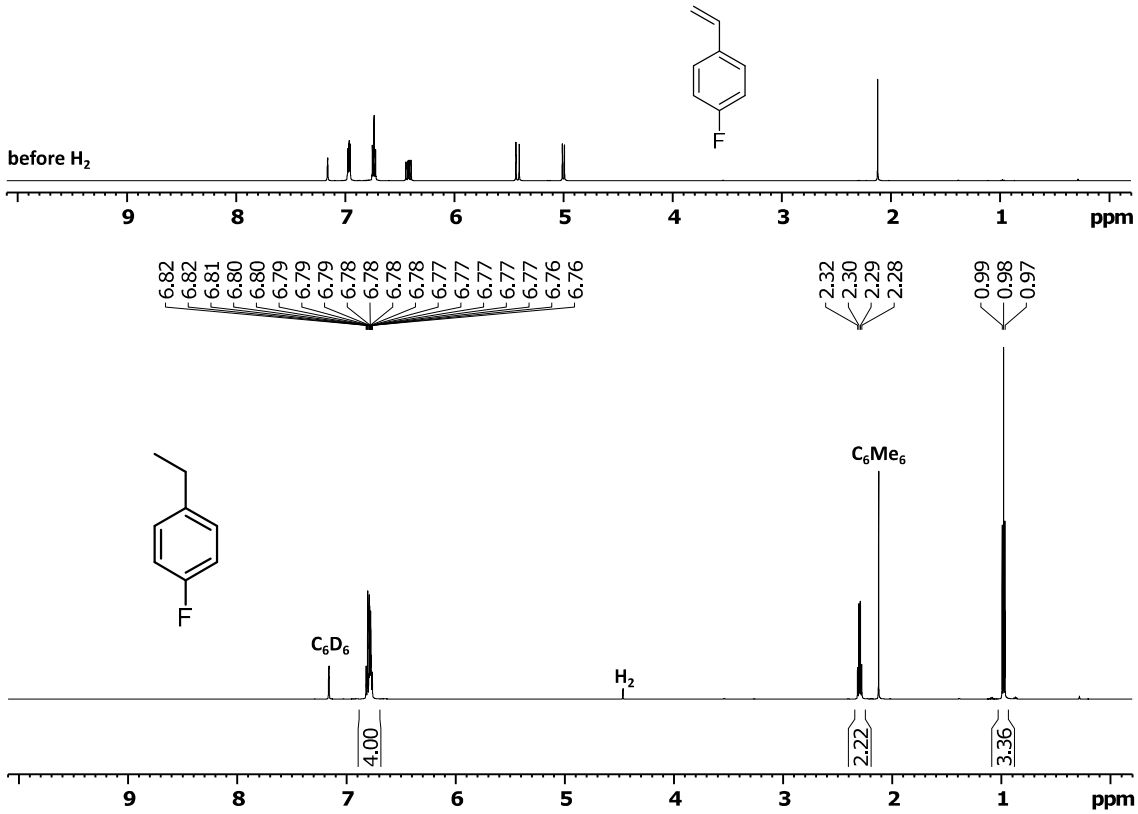

Figure S1. ^{1}H NMR spectrum (600 MHz, C_6D_6 / THF-d_8) of the hydrogenation of 1-ethenyl-4-fluorbenzene (**3**) before (top) and after (bottom) the addition of 7 bar H_2.

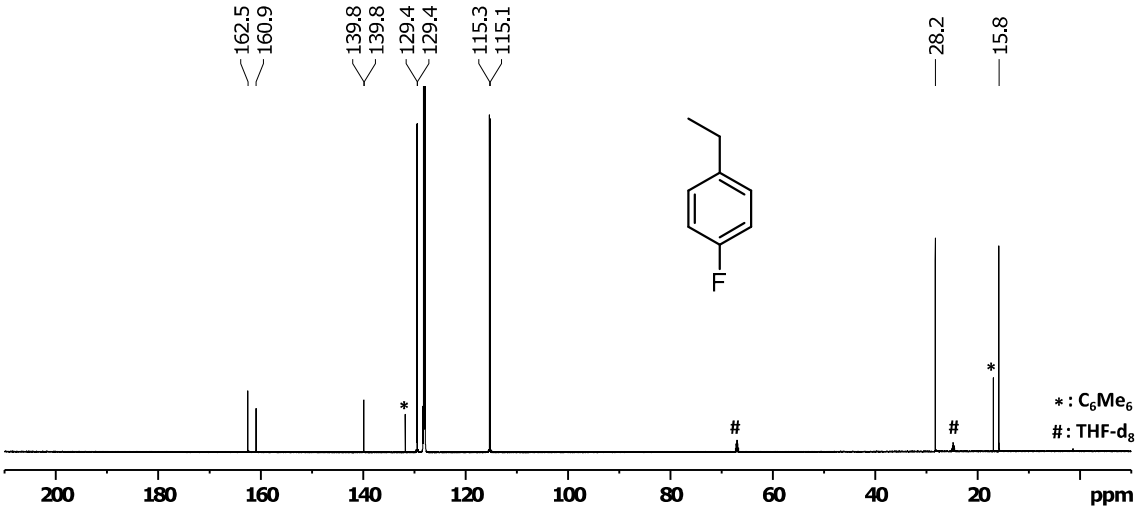

Figure S2. $^{13}C\{^{1}H\}$ NMR spectrum (151 MHz, C_6D_6 / THF-d_8) of 1-ethyl-4-fluorbenzene.

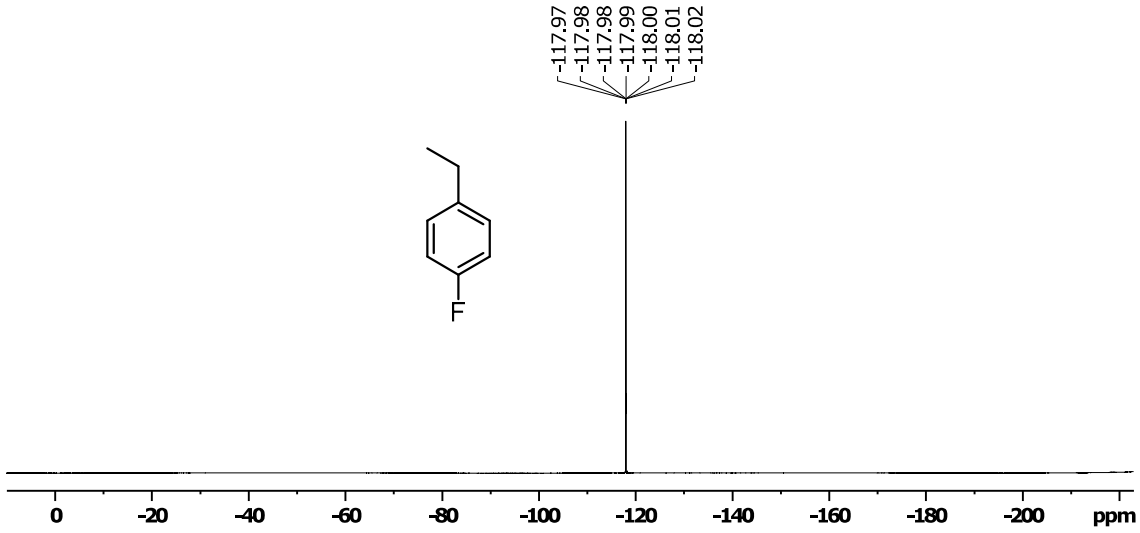

Figure S3. ^{19}F NMR spectrum (565 MHz, C_6D_6 / THF-d_8) of 1-ethyl-4-fluorbenzene.

Ethylbenzene

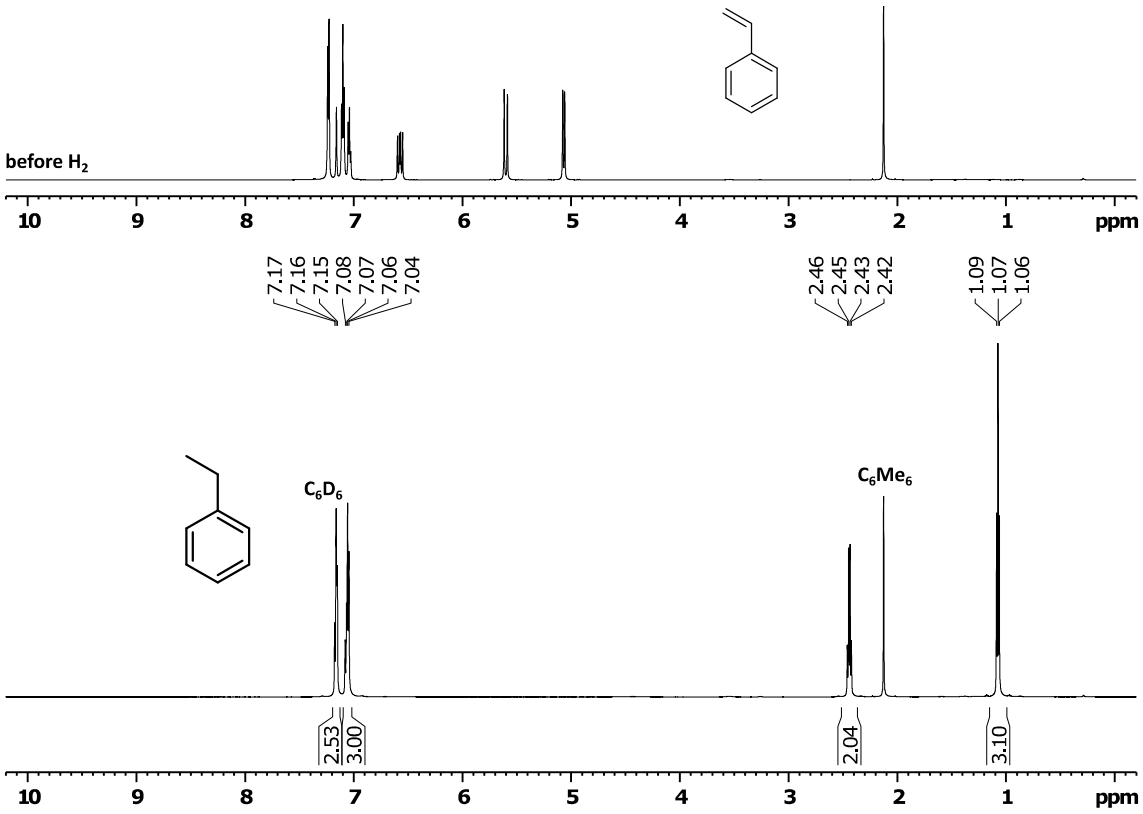

Figure S4. ^{1}H NMR spectrum (600 MHz, C_6D_6 / THF-d_8) of the hydrogenation of styrene (**4**) before (top) and after (bottom) the addition of 7 bar H_2.

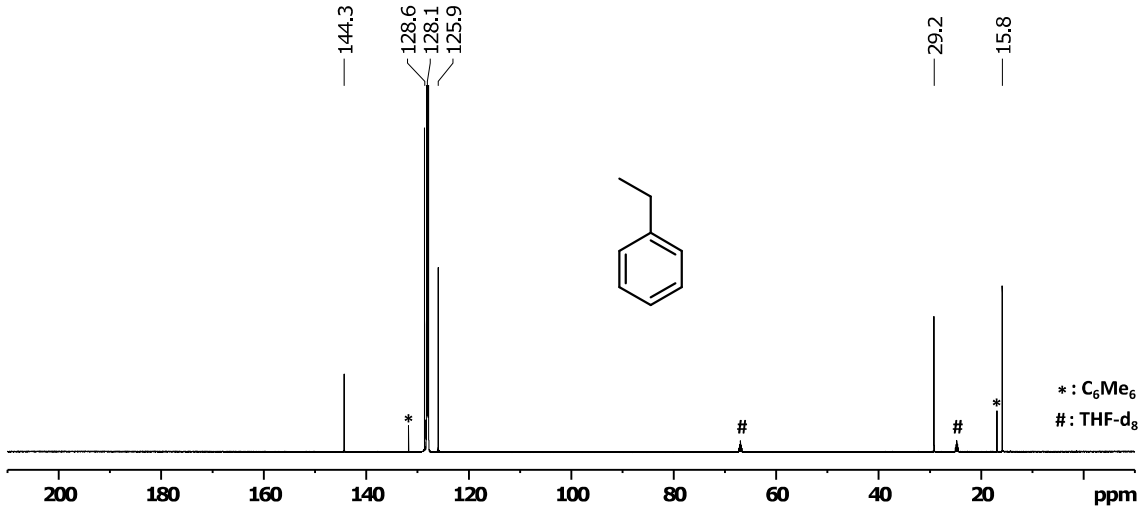

Figure S5. $^{13}C\{^{1}H\}$ NMR spectrum (151 MHz, C_6D_6 / THF-d_8) of ethylbenzene.

1-Ethyl-4-methoxybenzene

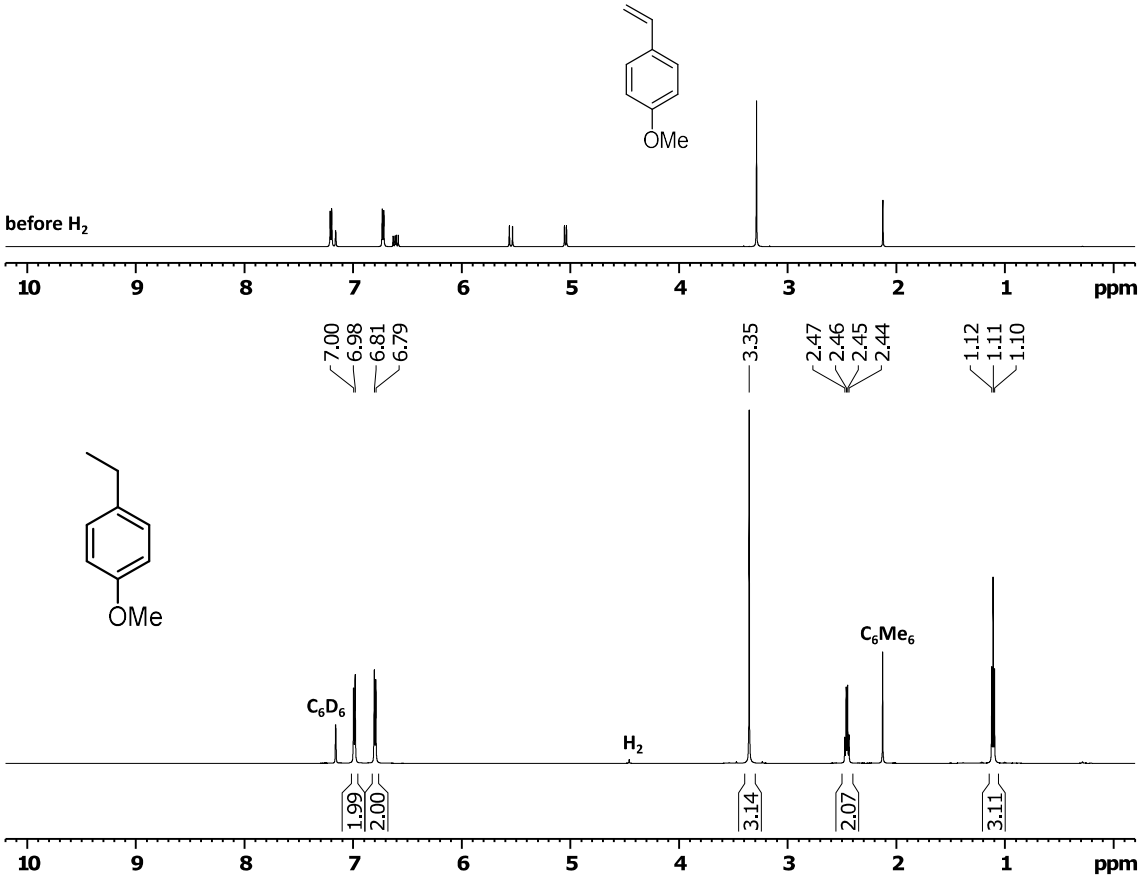

Figure S6. ^{1}H NMR spectrum (600 MHz, C_6D_6 / THF-d_8) of the hydrogenation of 1-ethenyl-4-methoxybenzene (**5**) before (top) and after (bottom) the addition of 7 bar H_2.

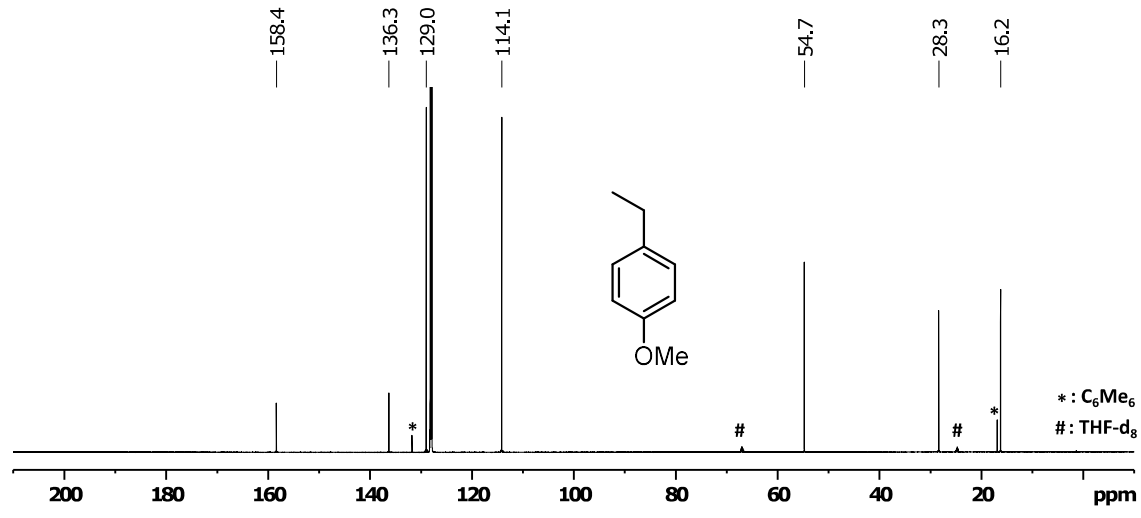

Figure S7. $^{13}C\{^{1}H\}$ NMR spectrum (151 MHz, C_6D_6 / THF-d_8) of 1-ethyl-4-methoxybenzene.

1-Ethyl-2-fluorobenzene

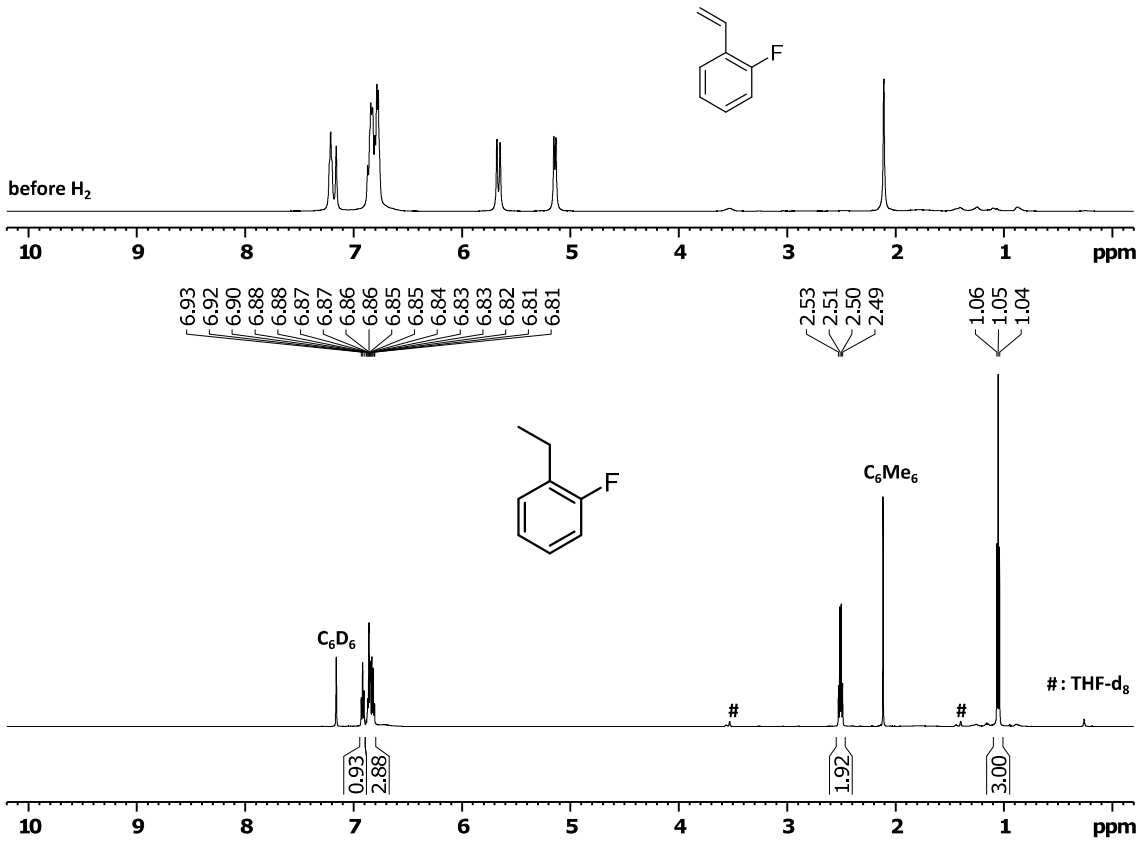

Figure S8. ^{1}H NMR spectrum (600 MHz, C_6D_6 / THF-d_8) of the hydrogenation of 1-ethenyl-2-fluorbenzene (**6**) before (top) and after (bottom) the addition of 7 bar H_2.

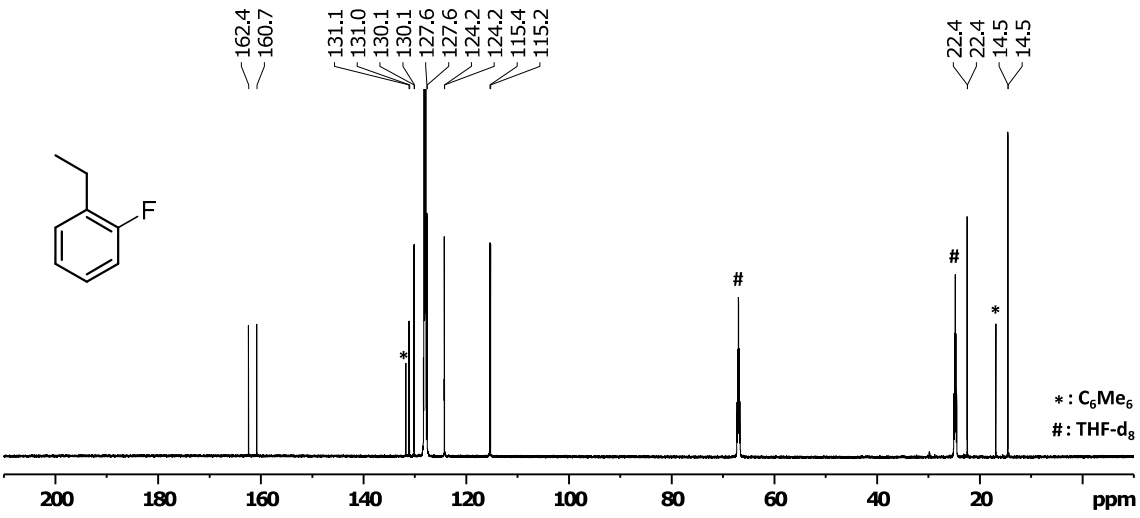

Figure S9. $^{13}C\{^1H\}$ NMR spectrum (151 MHz, C_6D_6 / THF-d_8) of 1-ethyl-2-fluorbenzene.

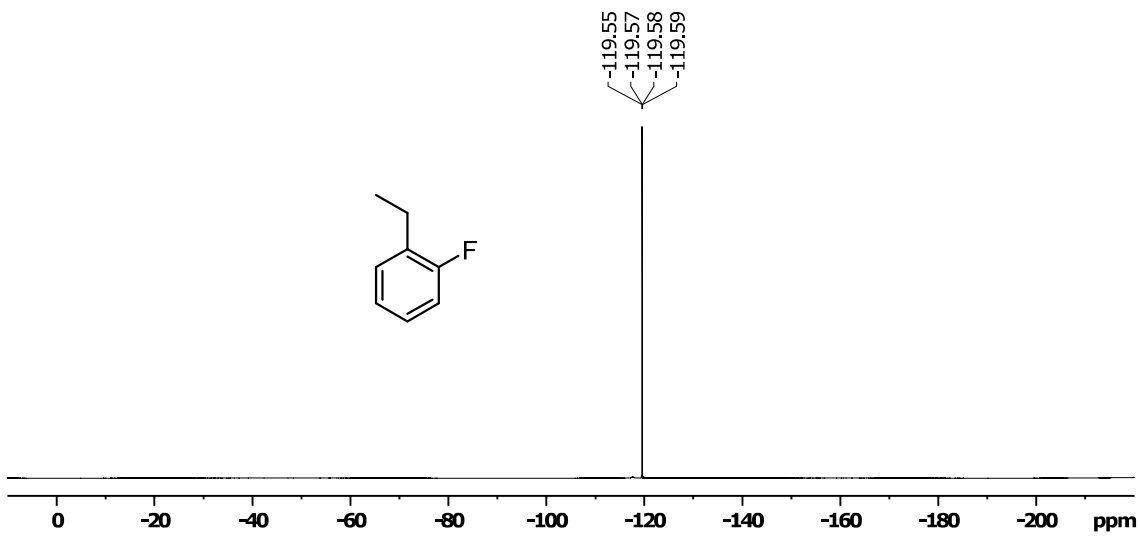

Figure S10. ^{19}F NMR spectrum (565 MHz, C_6D_6 / THF-d_8) of 1-ethyl-2-fluorbenzene.

Ethylcyclohexane

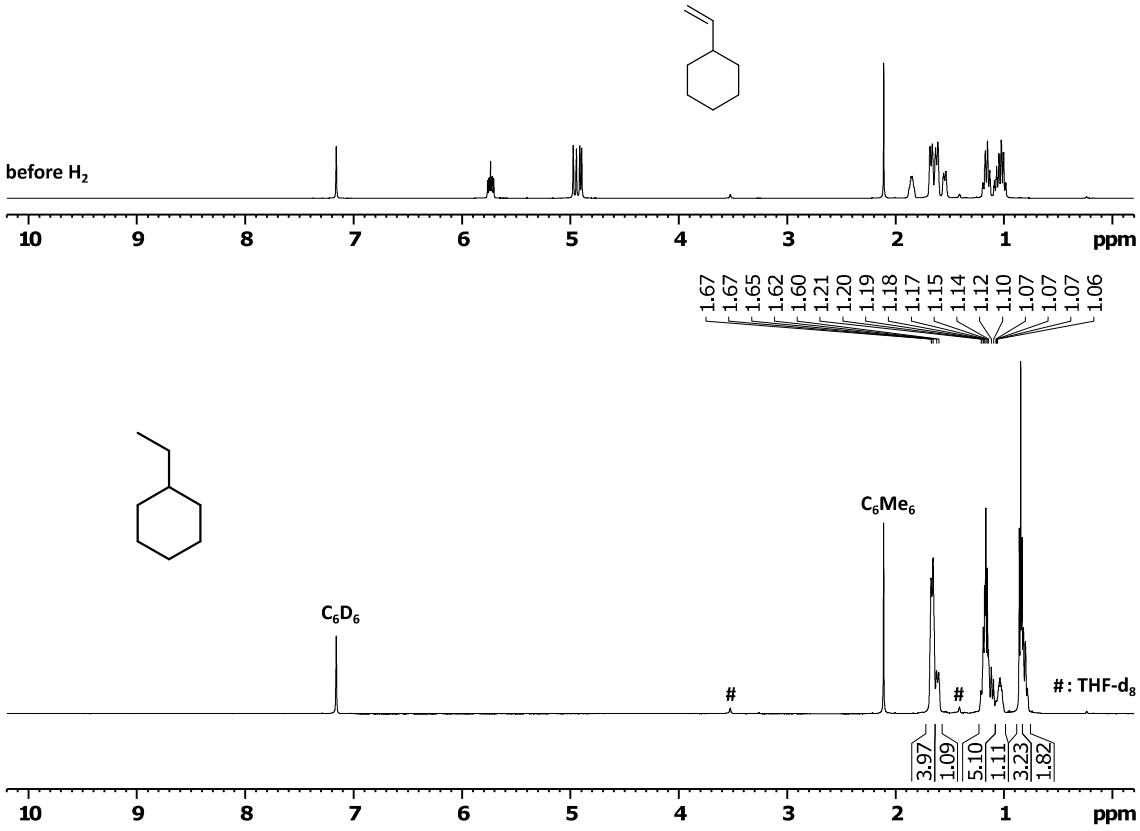

Figure S11. ^{1}H NMR spectrum (600 MHz, C_6D_6 / THF-d_8) of the hydrogenation of vinylcyclohexane (**7**) before (top) and after (bottom) the addition of 7 bar H_2.

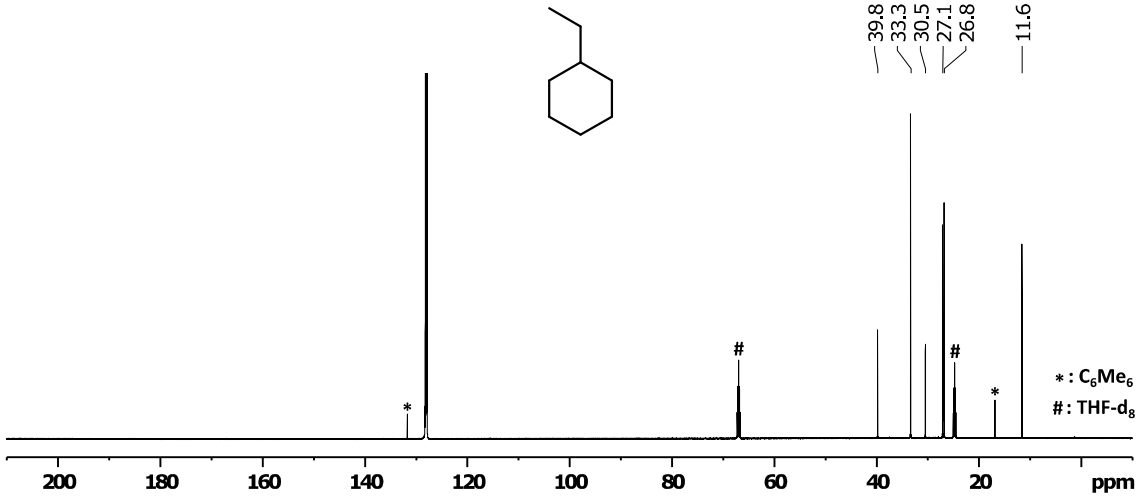

Figure S12. $^{13}C\{^1H\}$ NMR spectrum (151 MHz, C_6D_6 / THF-d_8) of ethylcyclohexane.

2,2-Dimethylbutane

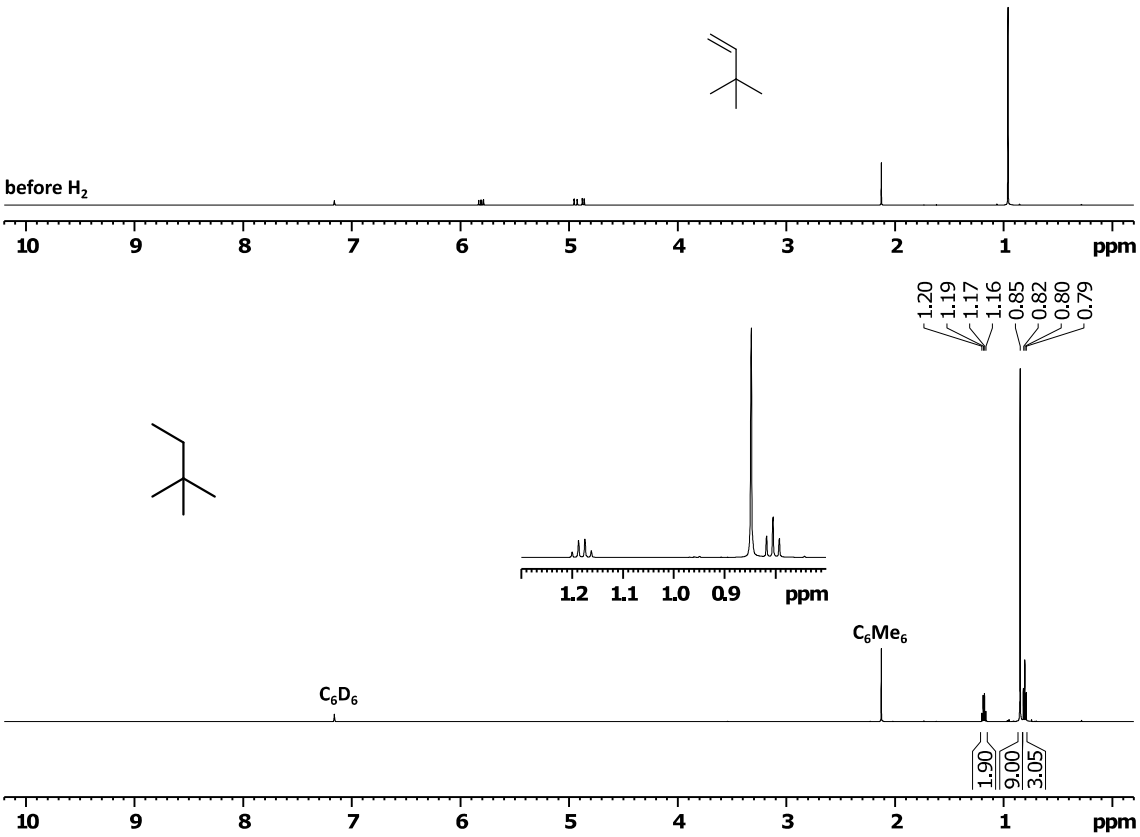

Figure S13. ^{1}H NMR spectrum (600 MHz, C_6D_6 / THF-d_8) of the hydrogenation of 3,3-dimethylbut-1-ene (**8**) before (top) and after (bottom) the addition of 7 bar H_2.

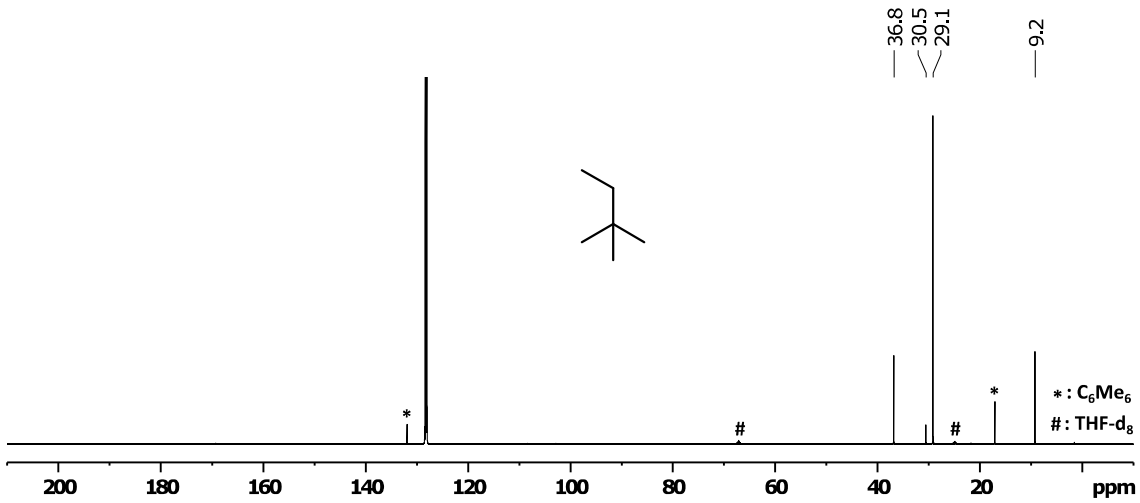

Figure S14. $^{13}C\{^1H\}$ NMR spectrum (151 MHz, C_6D_6 / THF-d_8) of2,2-dimethylbutane.

Isopropylbenzene

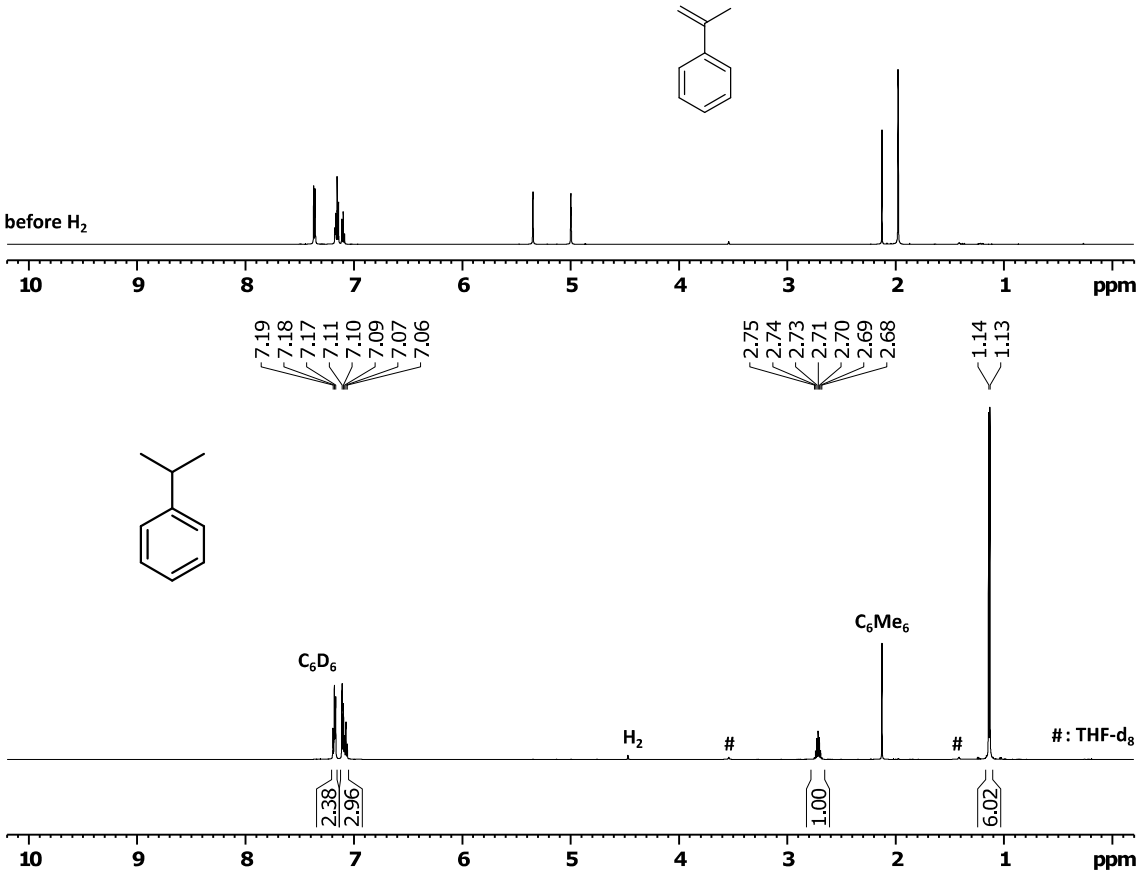

Figure S15. ^{1}H NMR spectrum (600 MHz, C_6D_6 / THF-d_8) of the hydrogenation of 2-phenylpropene (**9**) before (top) and after (bottom) the addition of 7 bar H_2.

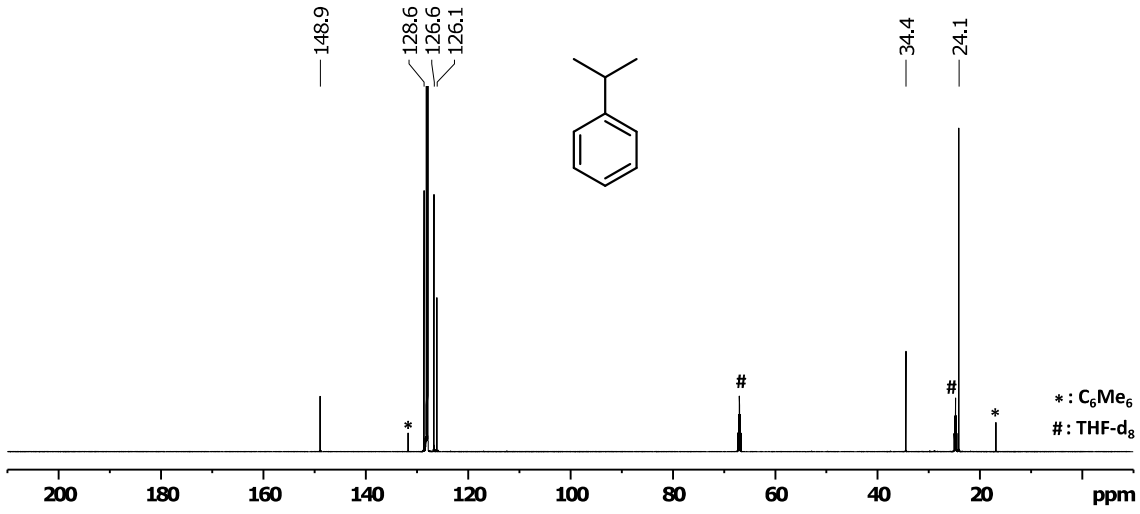

Figure S16. $^{13}C\{^1H\}$ NMR spectrum (151 MHz, C_6D_6 / THF-d_8) of isopropylbenzene.

Norbornane

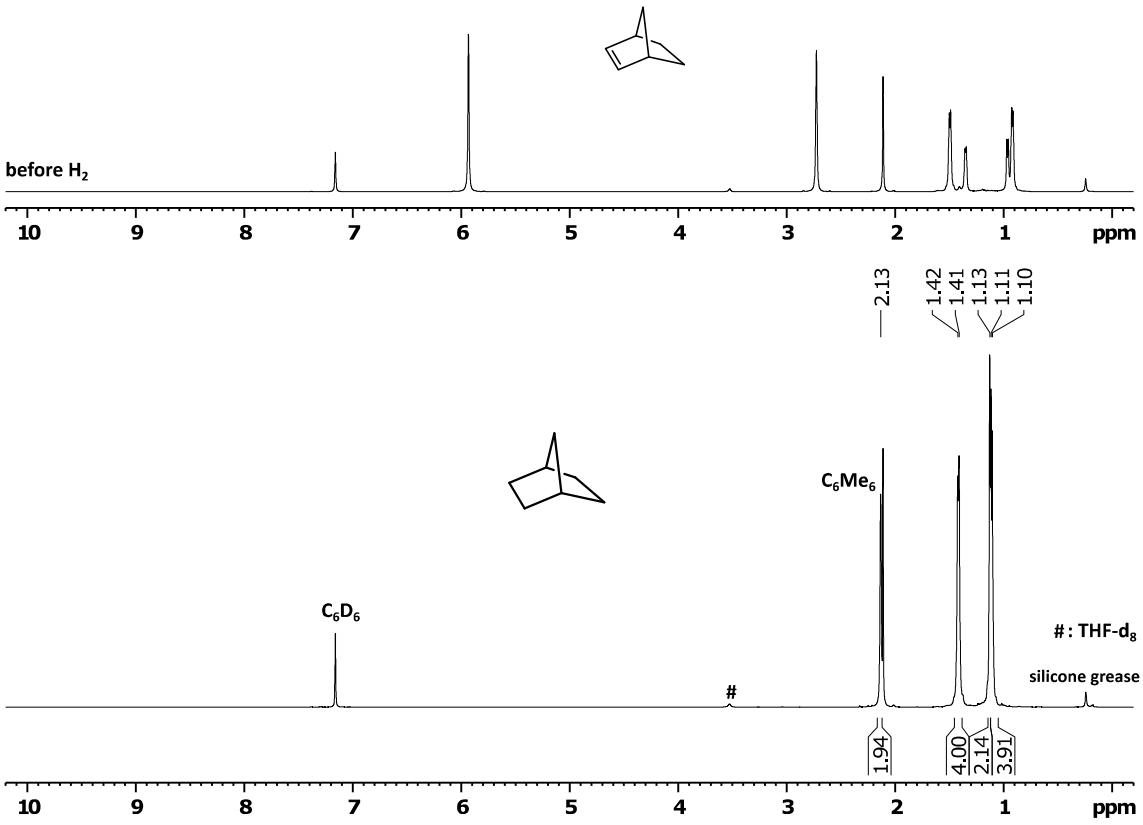

Figure S17. ^{1}H NMR spectrum (600 MHz, C_6D_6 / THF-d_8) of the hydrogenation of norbornene (**10**) in before (top) and after (bottom) the addition of 7 bar H_2.

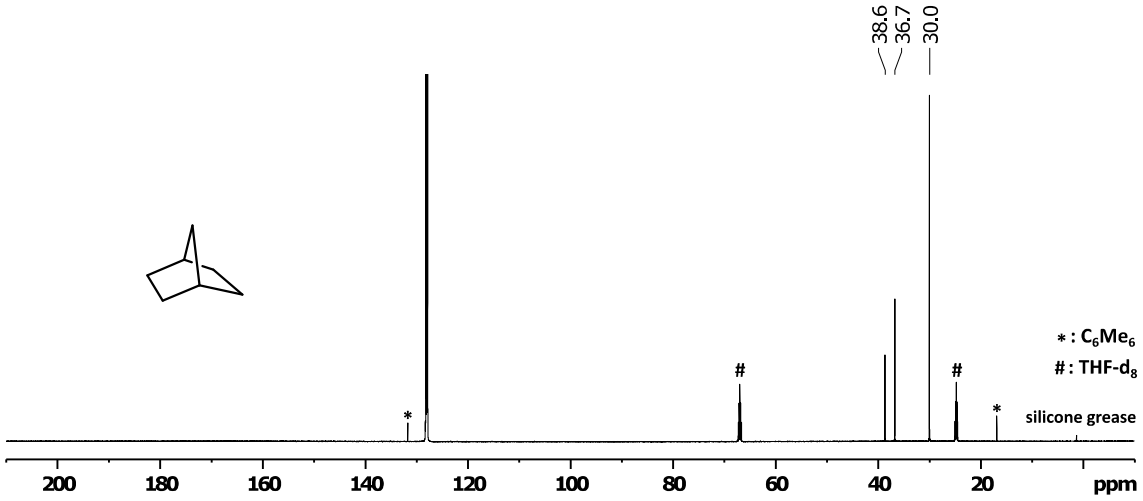

Figure S18. $^{13}C\{^1H\}$ NMR spectrum (151 MHz, C_6D_6 / THF-d_8) of norbornane.

4-Ethylcyclohexene and ethylcyclohexane

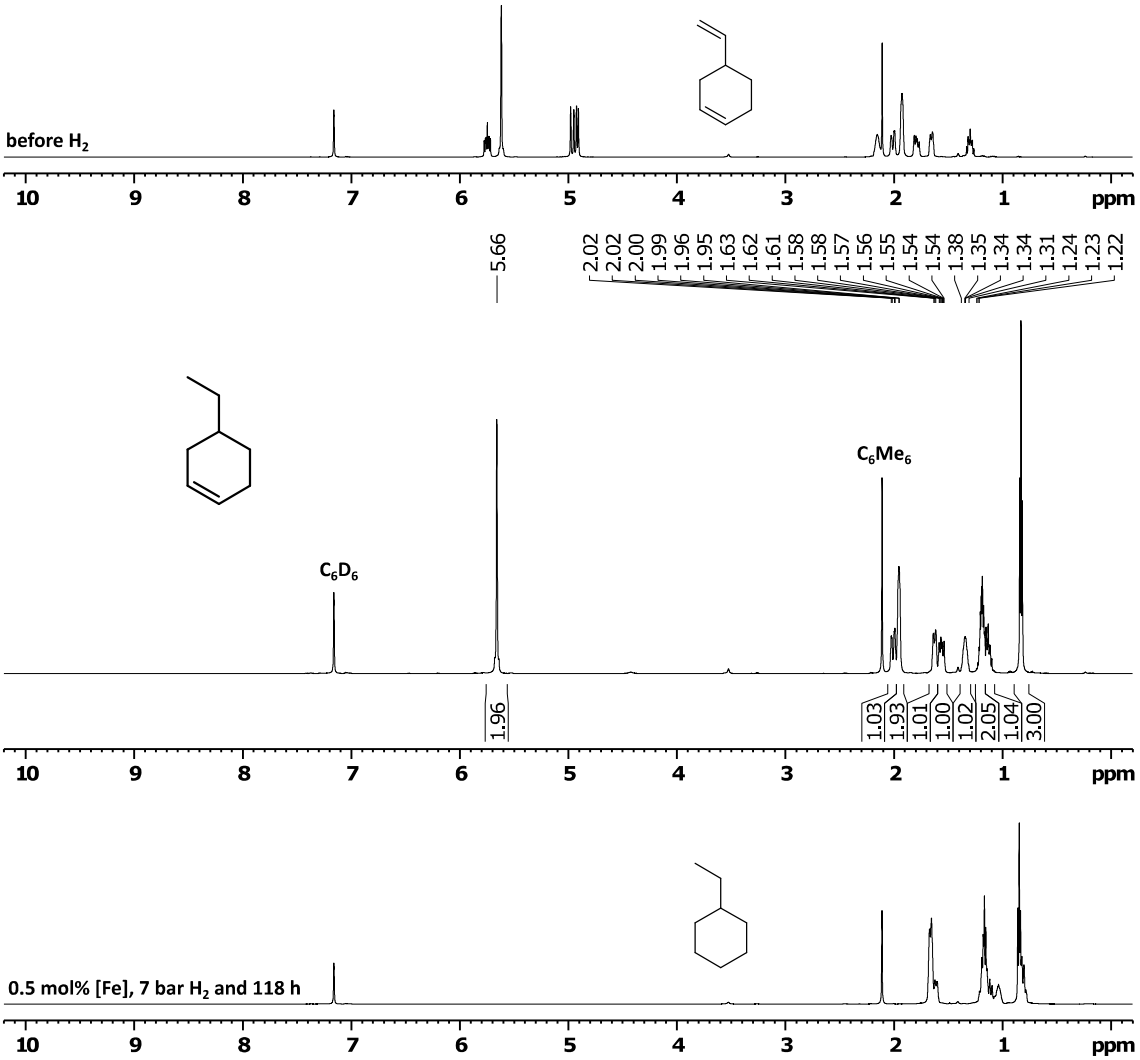

Figure S19. ^{1}H NMR spectrum (600 MHz, C_6D_6 / THF-d_8) of the hydrogenation of vinylcyclohexene (**11**) before (top) and after (middle) the addition of 7 bar H_2 and after 118 h (bottom).

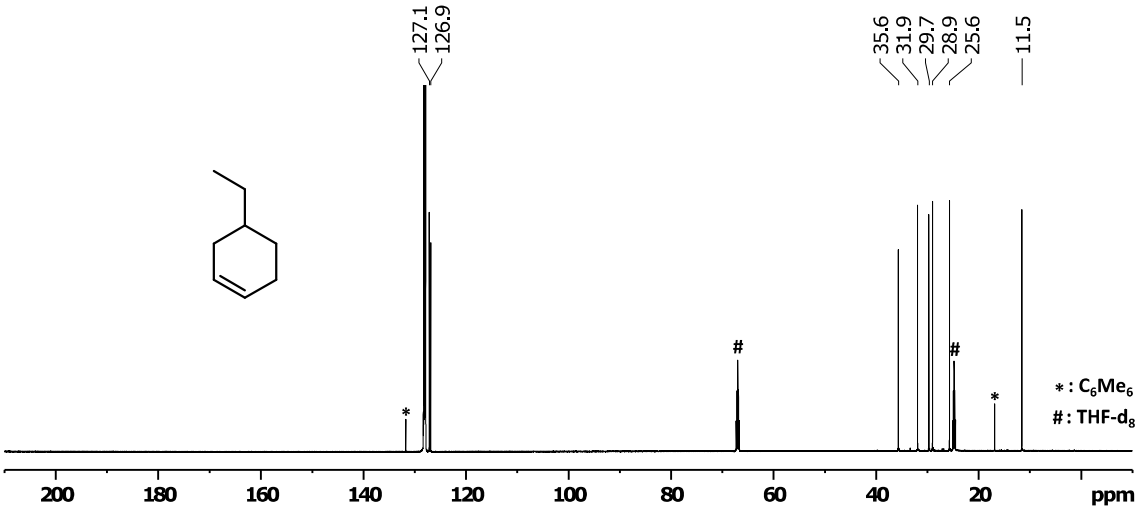

Figure S20. $^{13}C\{^{1}H\}$ NMR spectrum (151 MHz, C_6D_6 / THF-d_8) of 4-ethylcyclohexene.

(*E*)-But-1-en-1-ylbenzene and butylbenzene

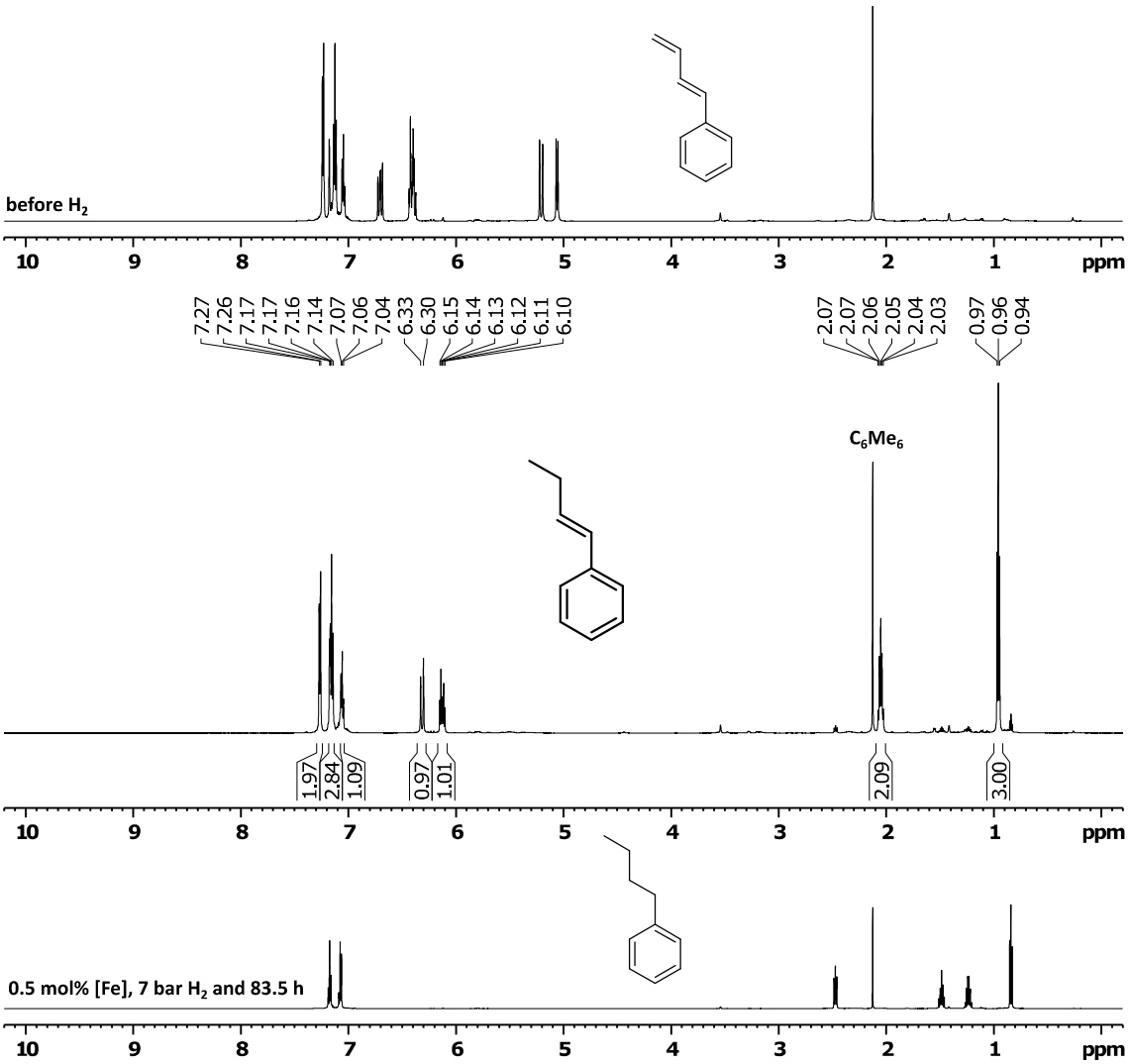

Figure S21. ^{1}H NMR spectrum (600 MHz, C_6D_6 / THF-d_8) of the hydrogenation of (*E*)-buta-1,3-dien-1-ylbenzene (**12**) in C_6D_6 before (top) and after (middle) the addition of 7 bar H_2 and after 83.5 h (bottom).

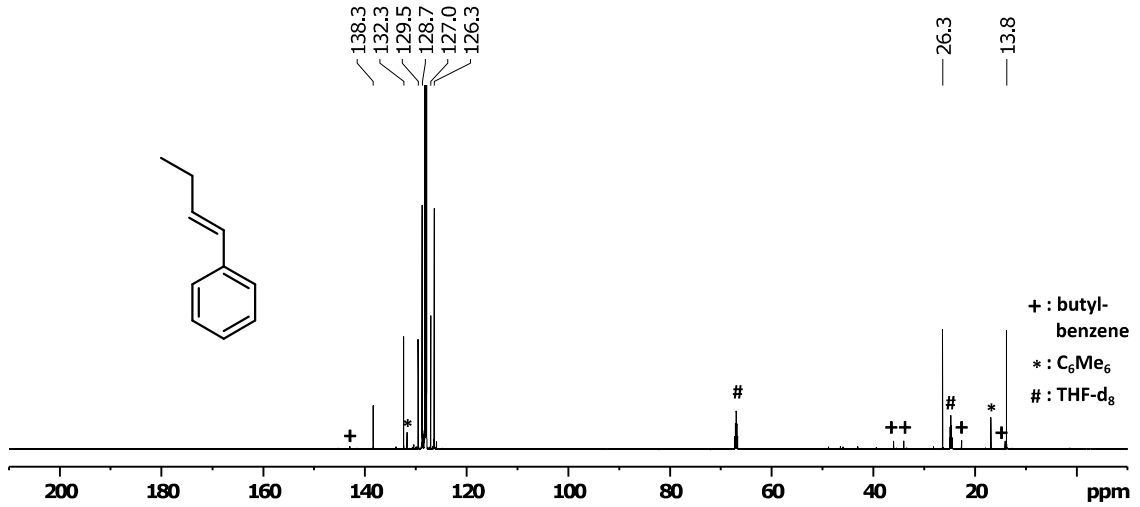

Figure S22. $^{13}C\{^1H\}$ NMR spectrum (151 MHz, C_6D_6 / THF-d_8) of (*E*)-but-1-en-1-ylbenzene.

Butylbenzene

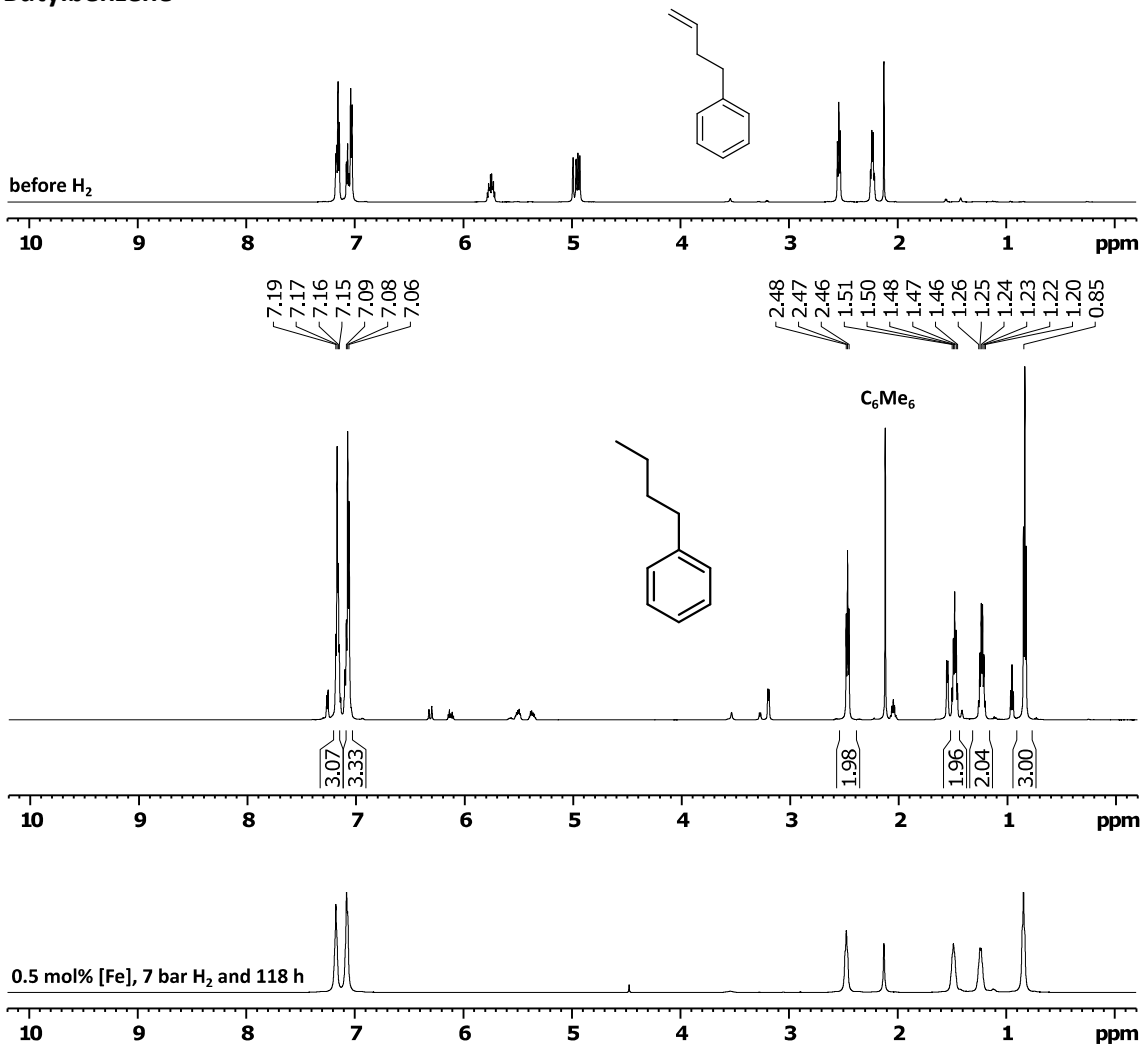

Figure S23. ^{1}H NMR spectrum (600 MHz, C_6D_6 / THF-d_8) of the hydrogenation of but-3-en-1-ylbenzene (**14**) in C_6D_6 before (top), after (middle) the addition of 7 bar H_2 and after 118 h (bottom).

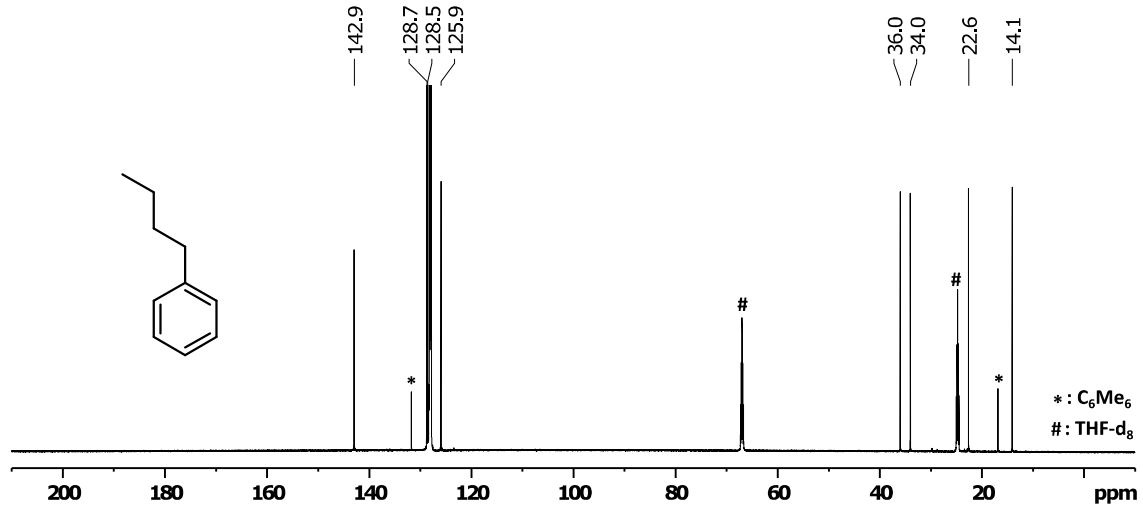

Figure S24. $^{13}C\{^1H\}$ NMR spectrum (151 MHz, C_6D_6 / THF-d_8) of butylbenzene.

Hexane

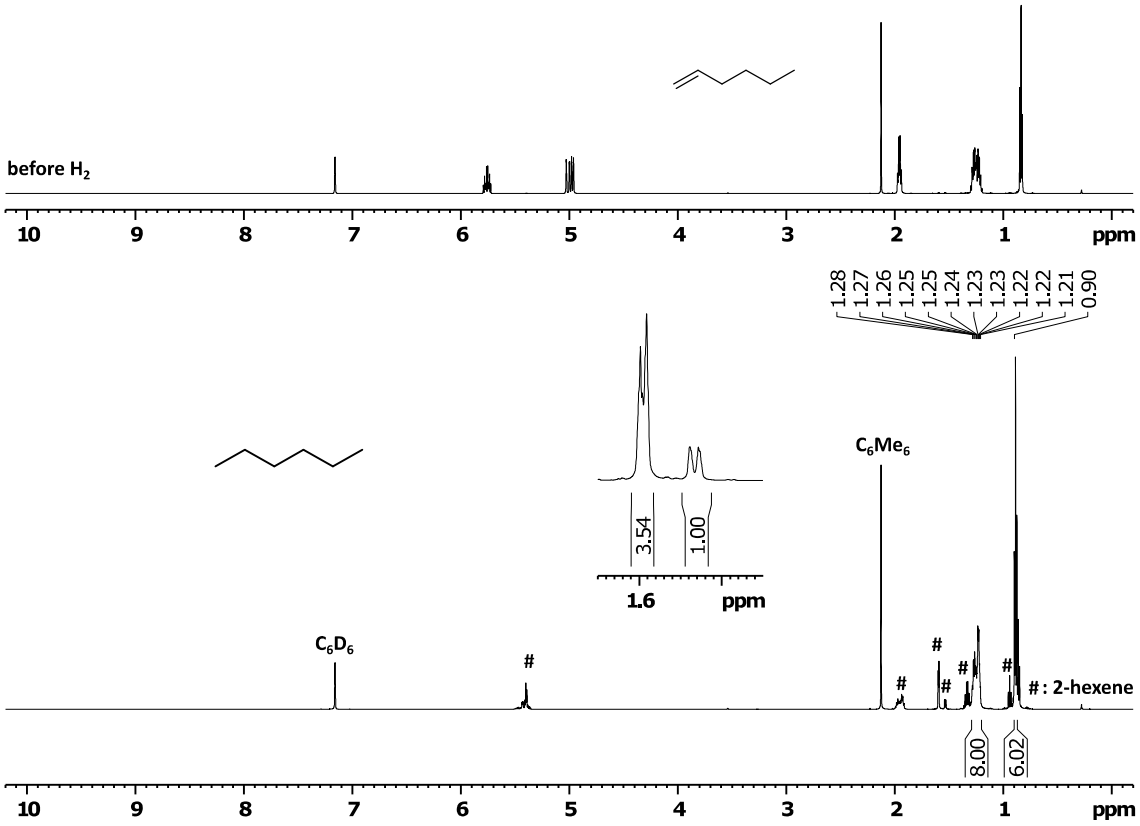

Figure S25. ^{1}H NMR spectrum (600 MHz, C_6D_6 / THF-d_8) of the hydrogenation of 1-hexene (**15**) in C_6D_6 before (top) and after (bottom) the addition of 7 bar H_2.

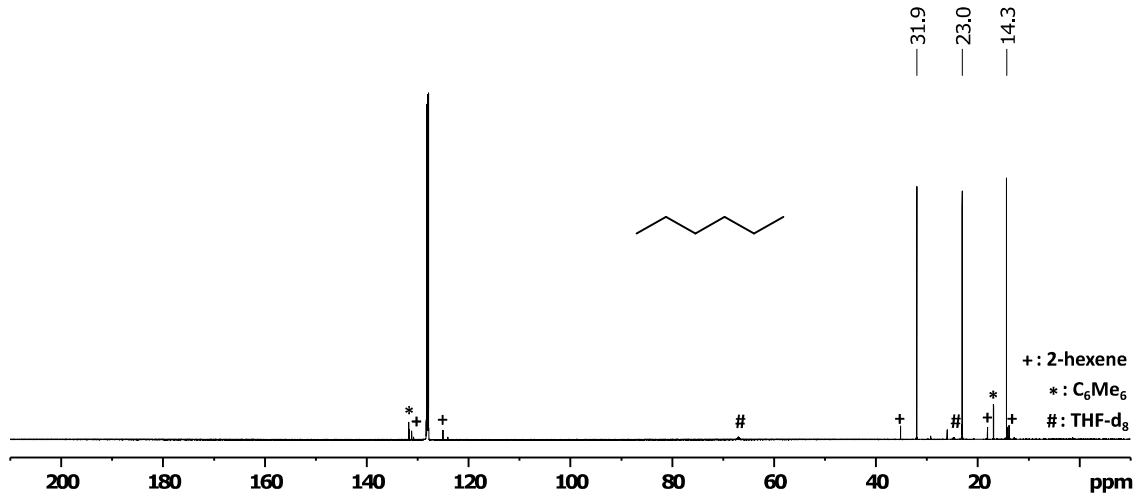

Figure S26. $^{13}C\{^1H\}$ NMR spectrum (151 MHz, C_6D_6 / THF-d_8) of hexane.

1.4 Challenging substrates

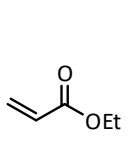

13

1.0 mol%
10 min
54% conversion

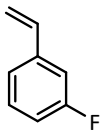

S1

1.0 mol%
rapid polymerisation

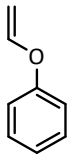

S2

0.1 mol%
no conversion

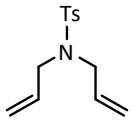

S3

0.1 mol%
no conversion

Ethyl acrylate

Following the general procedure ethyl acrylate (**13**) (18.32 mg,19.5 µL, 182.98 µmol) was hydrogenated with 1.0 mol% catalyst. The reaction showed 54 % conversion after 10 min of vigorous shaking.

The NMR data are in accordance with those previously reported.[12]

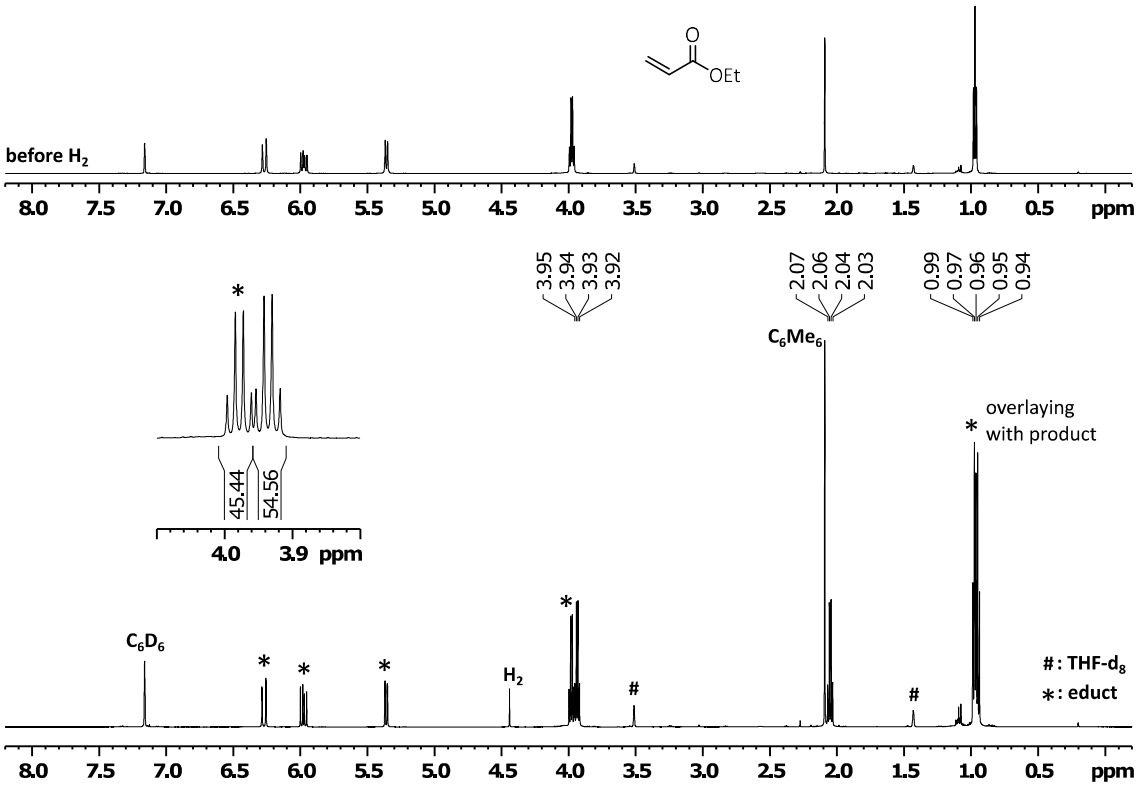

Figure S27. ^{1}H NMR spectrum (600 MHz, C_6D_6 / THF-d_8) of the hydrogenation of ethyl acrylate before (top) and after (bottom) the addition of 7 bar H_2.

1-Ethenyl-3-fluorobenzene

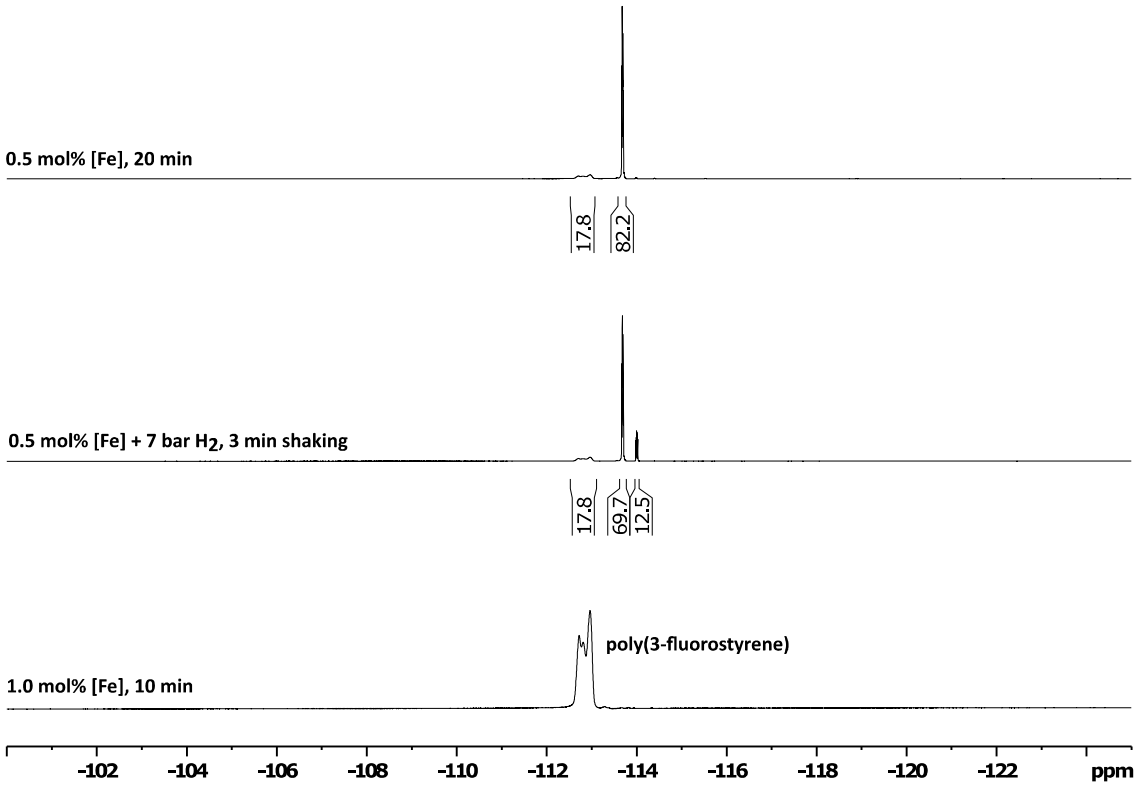

Figure S28. ^{19}F NMR spectrum (565 MHz, C_6D_6 / THF-d_8) of the hydrogenation of m-F-styrene (**S1**) with 0.5 mol% of **2** before (top) and after the addition of H_2 (middle) and of the mixture of 1.0 mol% of **2** with m-F-styrene after 10 min (bottom).

1.5 Supporting experiments for mechanistic proposal in reactions mediated by 2

1.5.1 Attempts to observe a σ-H_2 complex

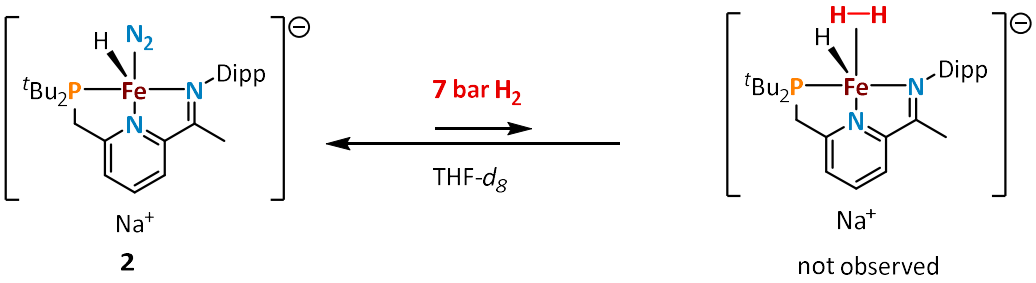

Placing THF-d_8 solutions of **2** under H_2 pressure (7 bar) did not produce any noticeable changes as inferred from ^{31}P and ^{1}H NMR spectroscopy, except a slight broadening of the ^{1}H resonances. Varying the temperature from −40 °C to +22 °C also did not cause any changes in the NMR spectra. Since the reaction of **2** with D_2 under the same conditions rapidly produces the corresponding deuteride,[1] we assume that if a σ-H_2 complex is formed, its concentration is undetectable by NMR spectroscopy.

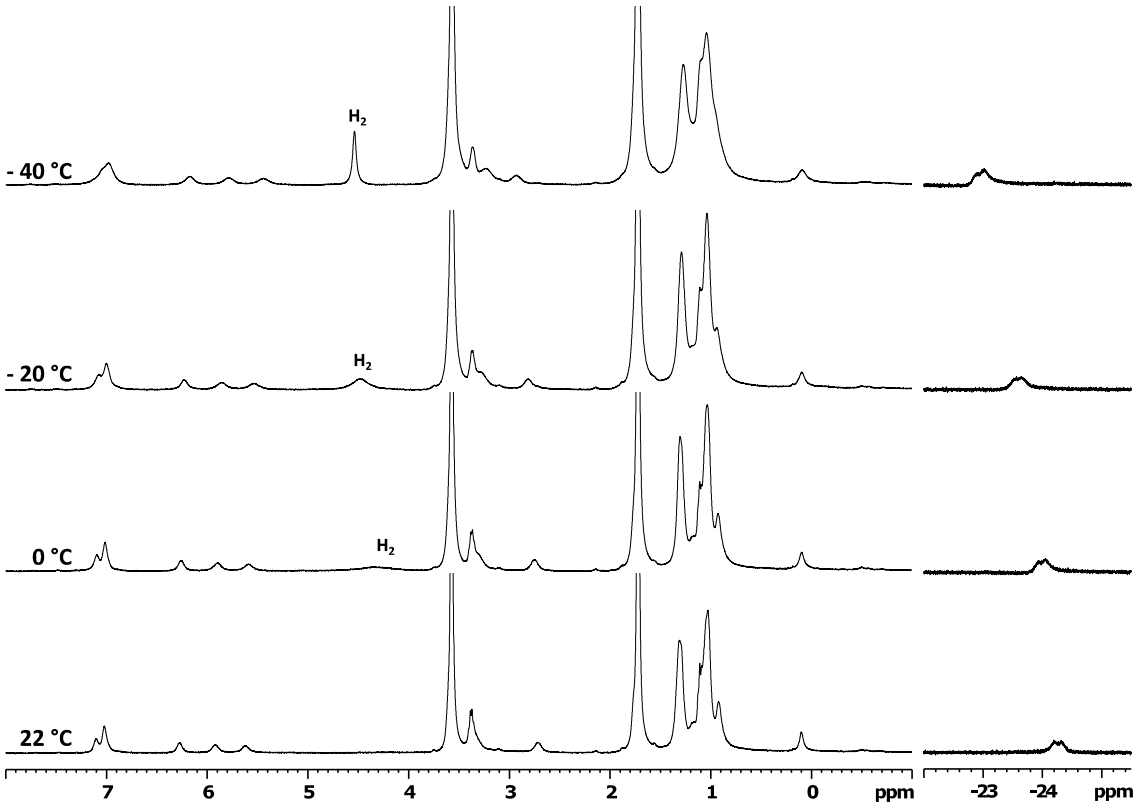

Figure S29. ^{1}H NMR spectrum (400 MHz, THF-d_8) of **2** at variable temperatures under H_2 pressure (7 bar). The spectrum between −22 ppm and −25.5 ppm is enlarged in comparison to the spectrum from 8 ppm to −1 ppm.

1.5.2 Attempts to observe an η^2-iron π-(p-F-styrene) complex

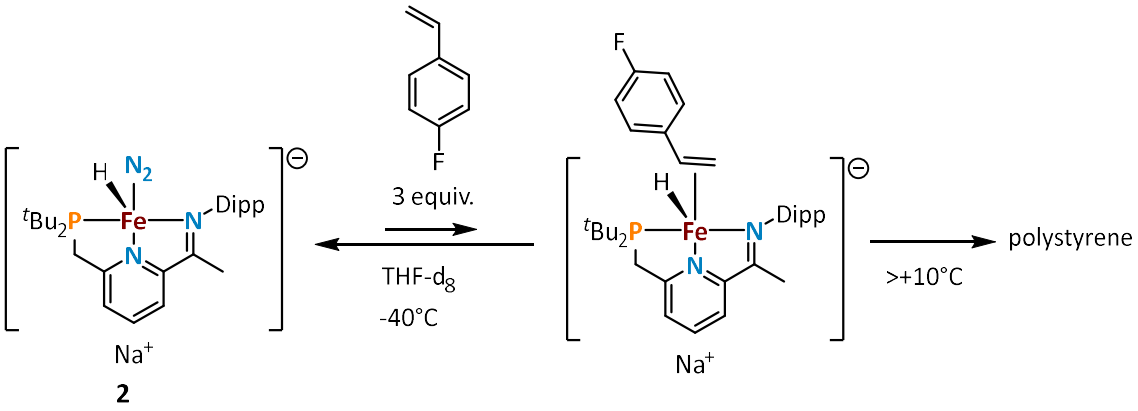

Mixing **2** and p-F-styrene **3** (3 equiv.) did not yield the expected η^2-iron π-(p-F-styrene) complex and left the starting materials unchanged at −40 °C as inferred from ^{1}H and ^{19}F NMR spectroscopy. Above +10 °C, styrene polymerisation could be observed (see below), suggesting that the π-complex is formed but does not accumulate in high enough concentrations that enable its detection by NMR spectroscopy.

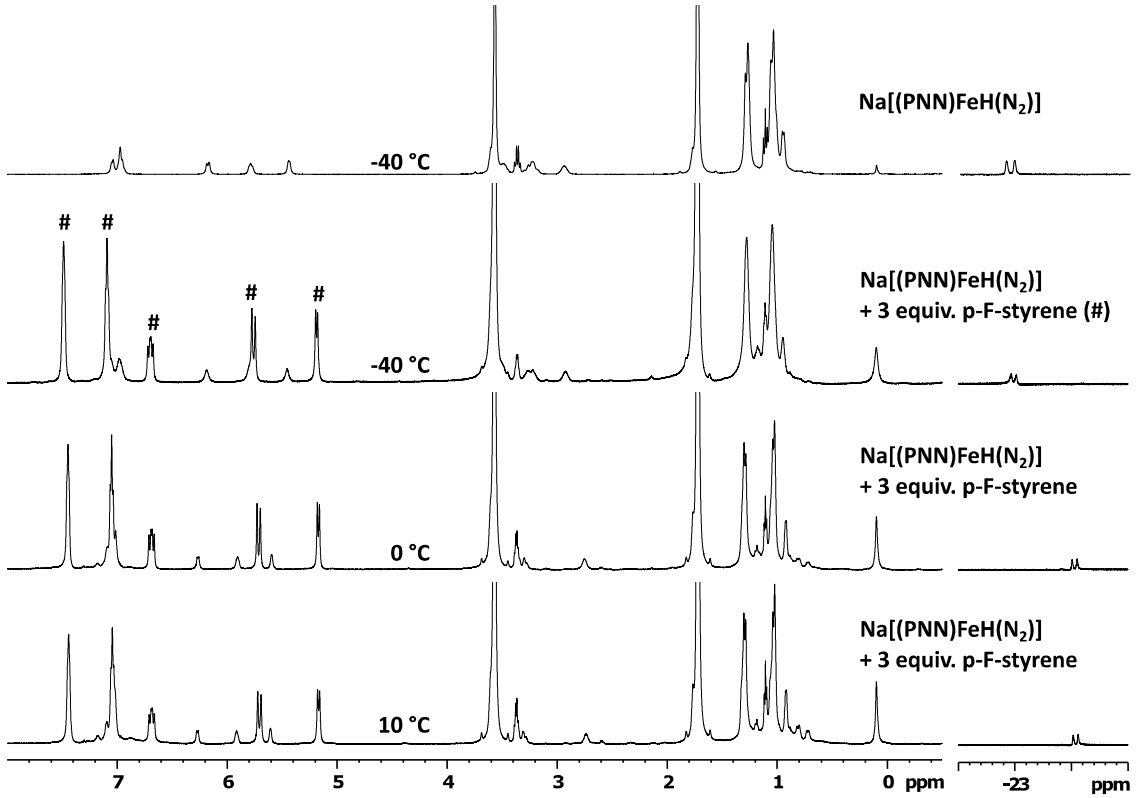

Figure S30. ^{1}H NMR spectrum (600 MHz, THF-d_8) of **2** at −40 °C (top) and with 3 equiv. of p-F-styrene **3** (added at −40 °C) at variable temperatures. The spectrum between −22 ppm and −25 ppm is enlarged in comparison to the spectrum from 8 ppm to −0.5 ppm.

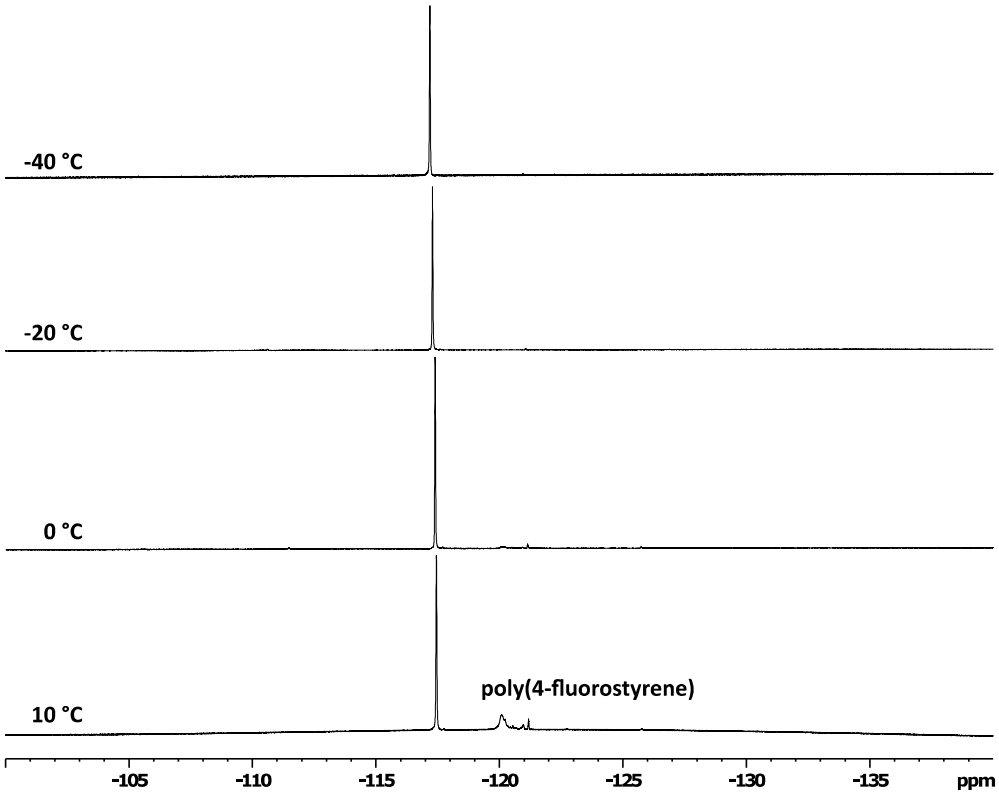

Figure S31. ^{19}F NMR spectrum (565 MHz, THF-d_8) of **2** with 3 equiv. of p-F-styrene **3** (added at −40 °C) at variable temperatures.

1.5.3 Deuteration Experiments

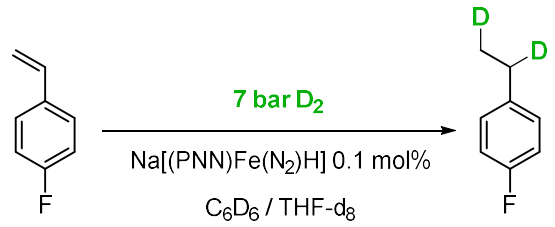

The hydrogenation of 1-ethenyl-4-fluorbenzene (**3**) was repeated using the hydride complex **2** as a catalyst under the standard catalytic conditions described in section 1.2, but with 7 bar of D_2 instead of H_2 and with non-deuterated solvents for one of the two experiments. The reaction led to the formation of the 1,2-deuterated product as judged by ^1H and $^2H\{^1H\}$ NMR spectroscopy (see spectra below).

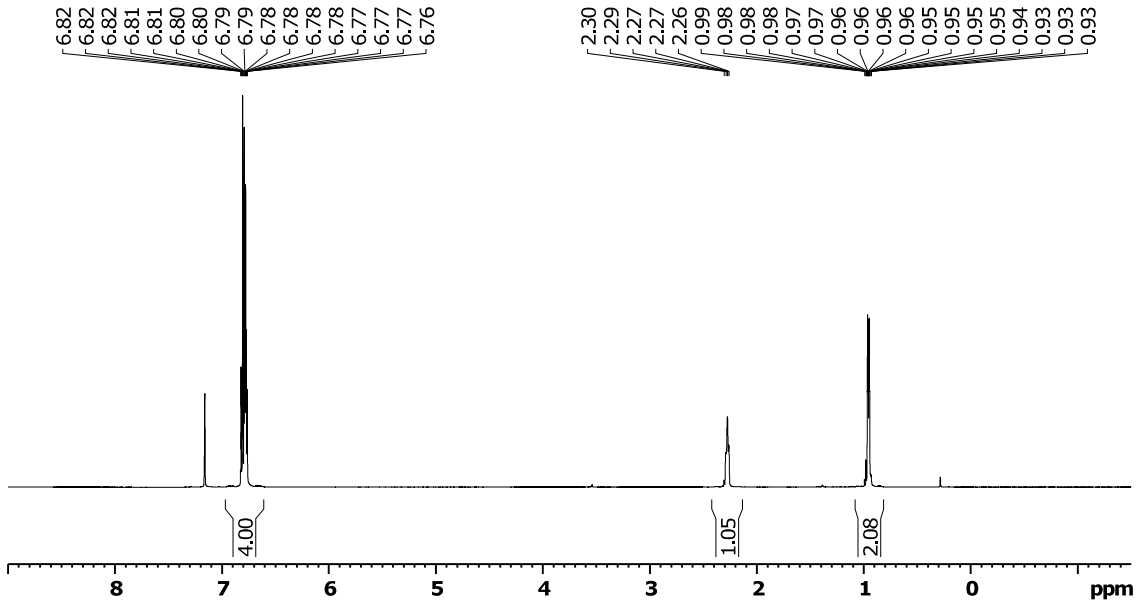

Figure S32. ^1H NMR spectrum (600 MHz, C_6D_6 / THF-d_8) of the hydrogenation (standard catalytic conditions) of 1-ethenyl-4-fluorbenzene (**3**) after the addition of 7 bar D_2.

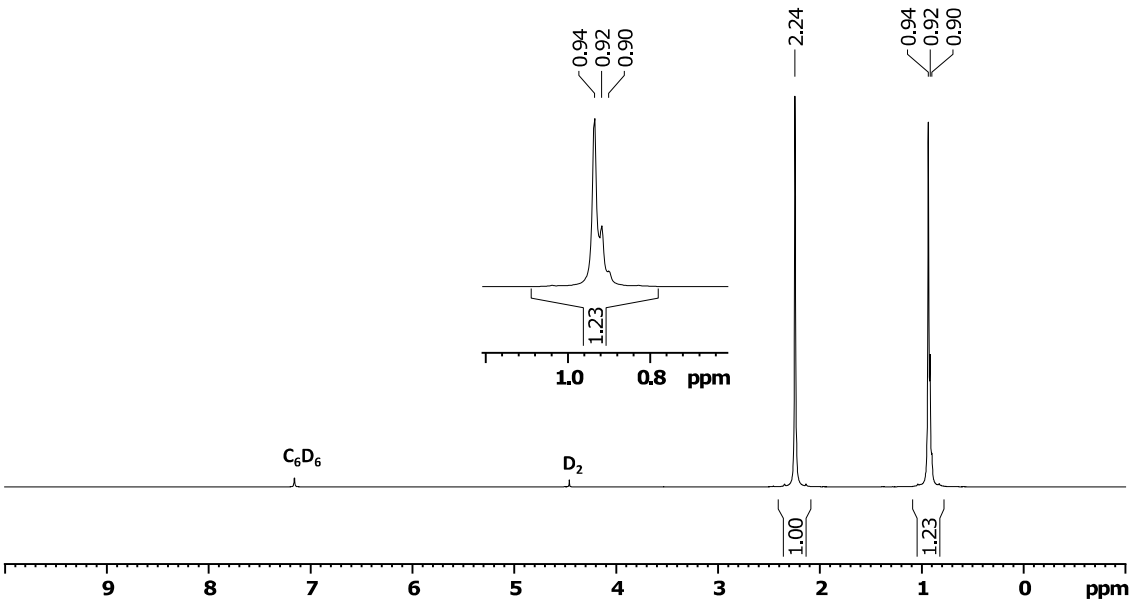

Figure S33. $^{2}H\{^{1}H\}$ NMR spectrum (600 MHz, C_6H_6 / THF) of the hydrogenation (standard catalytic conditions) of 1-ethenyl-4-fluorbenzene (**3**) after the addition of 7 bar D_2.

For the methyl resonance, the ^{2}H NMR spectrum shows the presence of two small shoulders at 0.92 and 0.90 ppm, and the integral value (1.2) is slightly higher than the expected value of 1, with respect to the neighbouring CHD resonance. We assign this phenomenon to the formation of small amounts of the CD_2H and CD_3 isotopomers, in addition to the expected CH_2D. The formation of these species suggests a reversibility of the insertion step (Figure 4, Manuscript), which, coupled with a fast H/D exchange from the iron hydride, leads to the formation of the observed isotopomers.

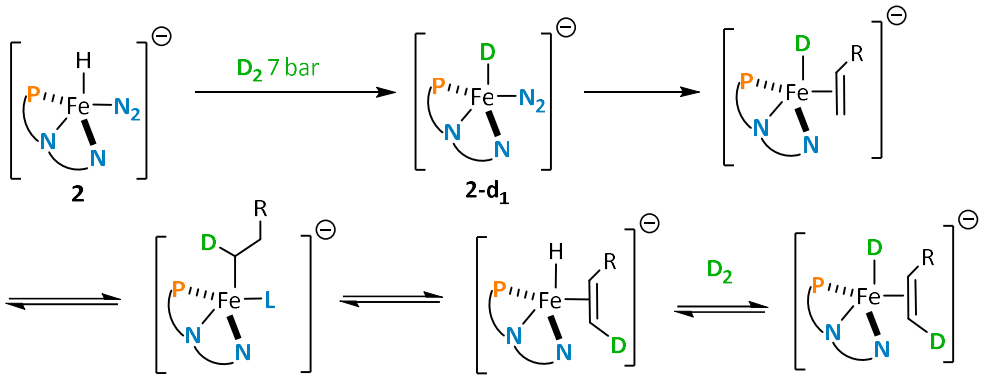

Figure S34. Proposed elementary steps in the catalytic cycle accounting for the formation of the small amounts of observed isotopomers.

1.6 Proposed mechanism for the hydrogenation reaction mediated by 1

Based on an analogously reported hydrogenation reaction based on pyrimidinediimine iron dinitrogen complexes,[13] we suggest a similar catalytic cycle for **1**. The cycle relies on the displacement of the labile N_2 ligand by an olefin (stronger π-acceptor), which renders the metal complex electron-rich enough to undergo facile oxidative addition of H_2. Insertion, followed by reductive elimination yields the hydrogenated product and regenerates the catalyst.

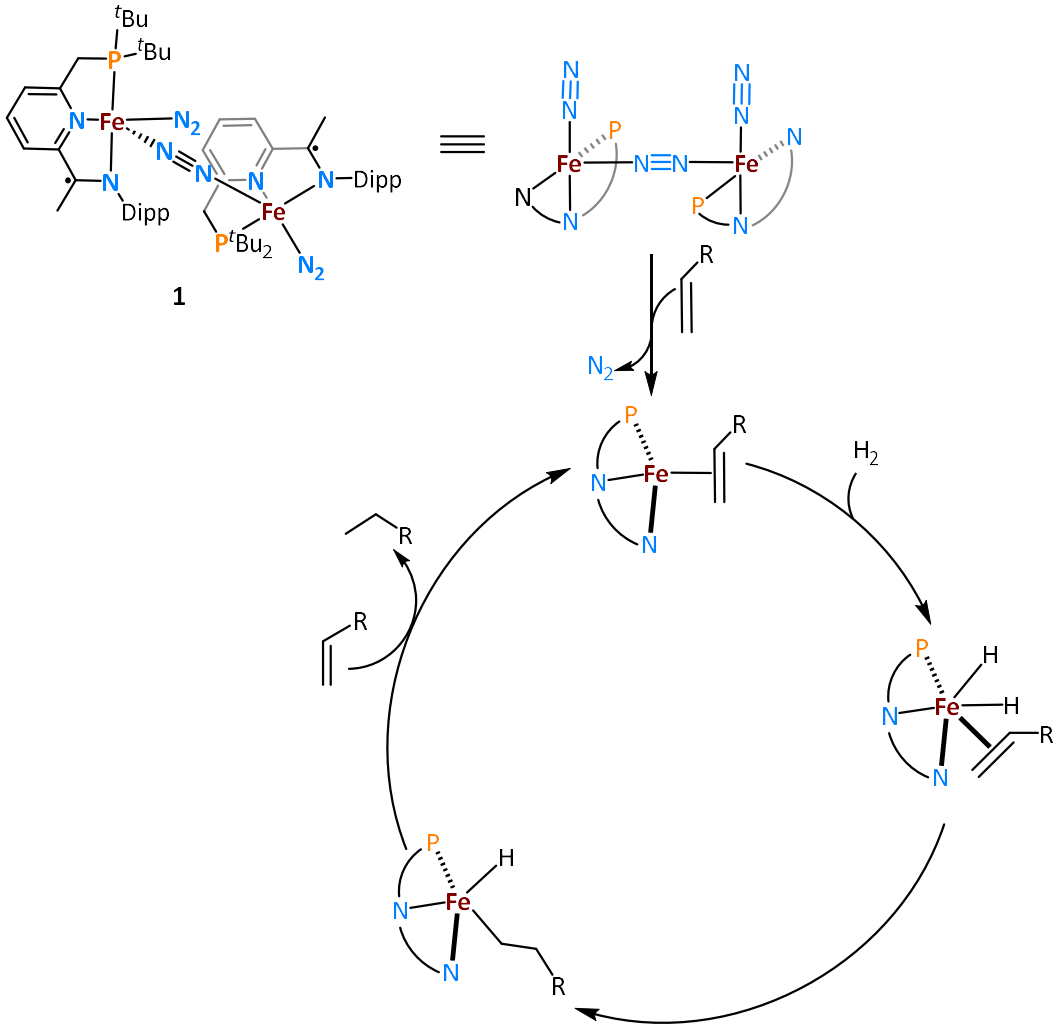

Figure S35. Proposed mechanism for olefin hydrogenation in the presence of **1**.

2 *Para*-Hydrogen studies

2.1 Sample preparation

All samples were prepared under an argon atmosphere in an MBraun glove box. For experiments with catalyst **1**, 4 mg of the catalyst were dissolved in 0.5 mL of the appropriate solvent, THF-d_8 or C_6D_6, in an Eppendorf tube and subsequently transferred to a 5 mm quick-pressure valve NMR tube (Wilmad). For experiments with o- or p-F-styrene as substrate, 100 µL of the appropriate substrate was added to the NMR tube.

In cases where **2** was employed as catalyst, 2 mg of the catalyst were dissolved in 0.5 mL of THF-d_8 and 50 µL of the appropriate substrate (o- or p-F-styrene) were added.

2.2 Experiments with gases

For precise regulation of the gases involved in the hydrogenation, a custom-built gas control system, as shown in **Figure S36.**, was employed. This system features a control panel (1) equipped with toggle switches that operate solenoid valves controlling the inlets for vacuum (2), thermal H_2 or pH_2 (3), and propene (4), and an outlet to the NMR tube (5). Details of this setup will be published elsewhere.

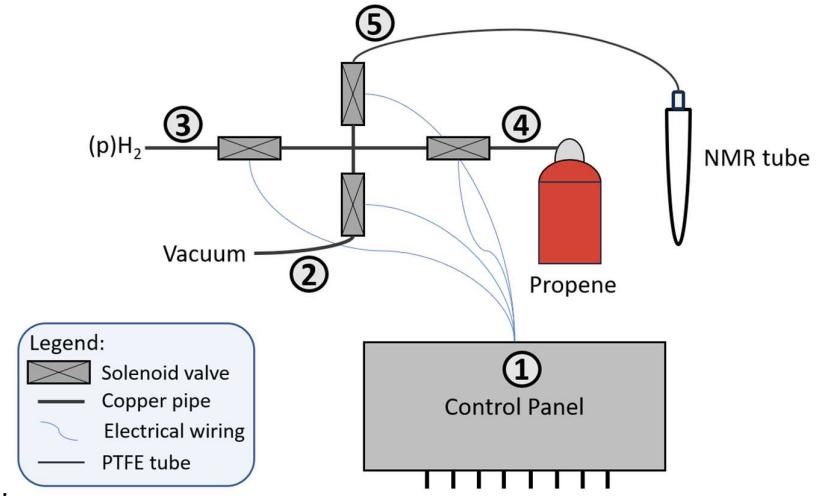

Figure S36. Scheme of the control panel (1) and the solenoid valves managing (p)H_2 (3), vacuum (2), propene (4) and the outlet (5) to the NMR tube.

A sealed NMR tube was connected to this system via a 1/16" PTFE tube. The pipes and tubes leading to the NMR tube were evacuated and flushed with the subsequently employed gas (propene or pH_2). This procedure was repeated three times to ensure removal of traces of oxygen.

For experiments involving propene as substrate, the NMR tube was then carefully opened and 2 bar of propene was introduced for 15 s while the tube was gently shaken. The tube was then sealed and shaken vigorously to ensure thorough mixing.

2.3 NMR-Experiments with para-hydrogen

The hydrogenation was then carried out at room temperature under ALTADENA[14,15] conditions in the earth magnetic field by addition of 4 bar of pH_2 to the sample tube for 10 s. After vigorous shaking of the sample tube for ca. 2 s, the sample was transferred to the magnetic field of a 1.4 Tesla Oxford benchtop spectrometer for radio frequency irradiation with a 90° pulse of 10.35 µs. Spectra were measured using a single scan.

After a waiting time, thermal spectra of each sample were recorded under identical conditions. Depending on the enhancement level and substrate, the waiting time ranged from 9 to 60 s after the acquisition of the PHIP spectrum.

2.4 Calculation and comparison of enhancement factors

The enhancement factor ε obtained in PHIP experiments is defined as the ratio between the intensity of a PHIP-enhanced signal and its corresponding signal in thermal equilibrium, each normalized by a suitable reference signal unaffected by PHIP. This relationship is shown in Eq. (1):

$$\frac{A_{S,PHIP}}{A_{S,therm}} = \varepsilon \times \frac{A_{Ref,PHIP}}{A_{Ref,therm}} \quad (1)$$

To determine the enhancement factor ε, the integral areas of the signal enhanced by PHIP ($A_{S,PHIP}$) and the corresponding thermal signal ($A_{S,ther}$) are compared. For ^{1}H NMR measurements using propene as substrate, the propane peak at 0.9 ppm was selected for evaluation. In experiments employing styrene derivatives, the signal at 2.5 ppm was utilized. To ensure comparability between spectra, a reference peak that remains unaffected by PHIP was employed, namely the solvent signal of THF-d_8 at 3.6 ppm or benzene at 7.2 ppm, respectively, depending on the solvent used in the experiment. Thus, $A_{Ref,PHIP}$ denotes the

area of reference signal in the enhanced spectrum while $A_{Ref,therm}$ denotes the area of the reference signal in the spectrum obtained at thermal equilibrium. The enhancement factor ε is then calculated according to Eq. (2):

$$\varepsilon = \frac{A_{S,PHIP}}{A_{S,therm}} \times \frac{A_{Ref,therm}}{A_{Ref,PHIP}} \quad (2)$$

In the ^{19}F NMR experiments using *o*-F-styrene and *p*-F-styrene as substrates, the resonance signals at −119.1 ppm (*o*-F-styrene) and −117.8 ppm (*p*-F-styrene) were employed for determination of $A_{S,PHIP}$ and $A_{S,therm}$. Since no reference peak was available here, the enhancement factor was calculated according to Eq. (3):

$$\varepsilon = \frac{A_{S,PHIP}}{A_{S,therm}} \quad (3)$$

The resulting enhancement factors of each experiment are summarized in **Table S1** below. The corresponding spectra are presented in the following **Figures S37-S50**.

Table S1. Enhancement factors measured in each experiment with catalysts **1** (ε_1) and **2** (ε_2).

Experiment / Substrate	ε_1	ε_2	Solvent
^{1}H Propene	280	50	THF-d_8
^{1}H p-F-Styrene	415	2250	THF-d_8
^{1}H p-F-Styrene	515		C_6D_6
^{1}H o-F-Styrene	1195	190	THF-d_8
^{1}H Styrene	845	170	THF-d_8
^{19}F p-F-Styrene	95	200	THF-d_8
^{19}F p-F-Styrene	775		C_6D_6
^{19}F o-F-Styrene	30	190	THF-d_8

The hydrogenation experiment with **1** and propene as substrate has been performed 3 times to calculate the standard deviation of the enhancement. Given the measured values of 270, 460, and 115, a relative standard deviation of 62.5% is obtained. This illustrates that a variety of parameters in the experimental setup (mixing times, magnetic field, substrate conversion rate, nature and spin states of reaction intermediates) significantly influences the obtained enhancement factors.

To compare ^{1}H signal enhancements acquired at different magnetic field strengths, spin polarisation must be considered. The thermal polarisation P_{th} is given by Eq. (4):[16]

$$P_{th} = tanh\left(\frac{\gamma\hbar B_0}{2k_B T}\right) \quad (4)$$

where γ is the gyromagnetic ratio of ^{1}H ($2.68 \cdot 10^8$ rad s^{-1} T^{-1}), B_0 the static field, k_B the Boltzmann constant, $\hbar$ the reduced Planck constant, and T the sample temperature (298 K). The polarisation generated by parahydrogen P_{Hyp} is obtained from the experimentally measured enhancement ε via Eq. (5):

$$P_{Hyp}[\%] = \varepsilon \cdot P_{th} \cdot 100\% \quad (5)$$

Applying this equation to the presented data, an enhancement of 2250 at 60 MHz (1.4 T) corresponds to a polarization of 1.09%. For comparison, an enhancement of 200 at 600 MHz (14.1 T) reported by Fout *et al.*[17] corresponds to a polarization of 0.97%. Thus, although the thermal polarisation is higher at 14.1 T, the much larger enhancement factor at 1.4 T compensates for it.

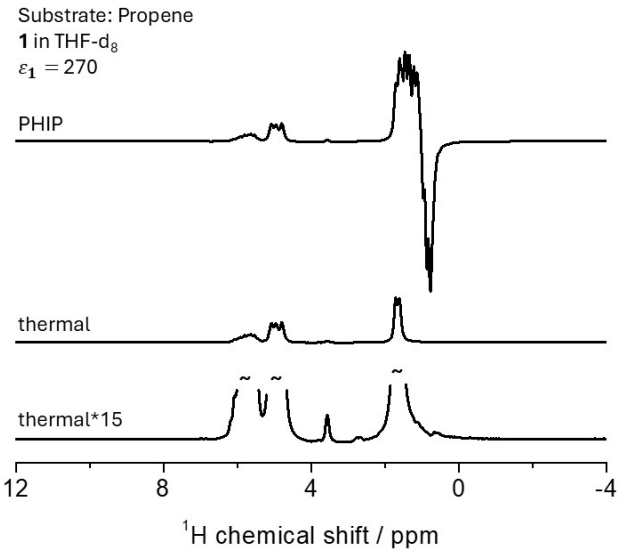

Figure S37. ^{1}H NMR spectra recorded during the hydrogenation of propene in THF-d_8 catalysed by **1**: (top) ^{1}H PHIP spectrum after the addition of pH_2, (middle) thermal spectrum after 40 s, and (bottom) 15-times enlarged thermal spectrum. The spectra are normalized to the solvent peak at 3.6 ppm.

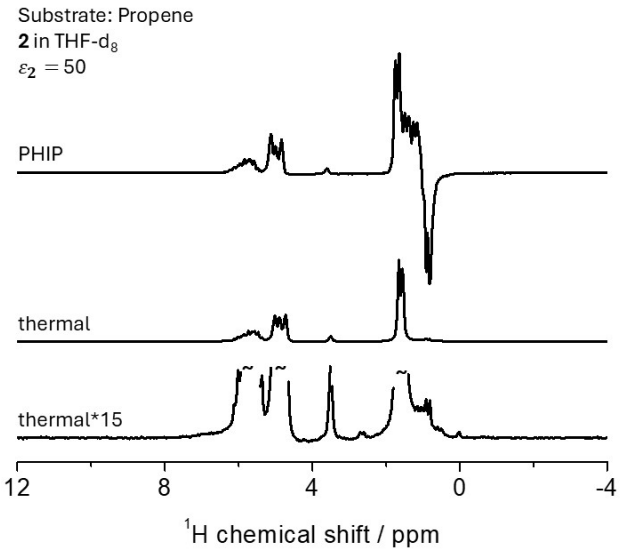

Figure S38. ^{1}H NMR spectra recorded during the hydrogenation of propene in THF-d_8 catalysed by **2**: (top) ^{1}H PHIP spectrum after the addition of pH_2, (middle) thermal spectrum after 12 s, and (bottom) 15-times enlarged thermal. The spectra are normalized to the solvent peak at 3.6 ppm.

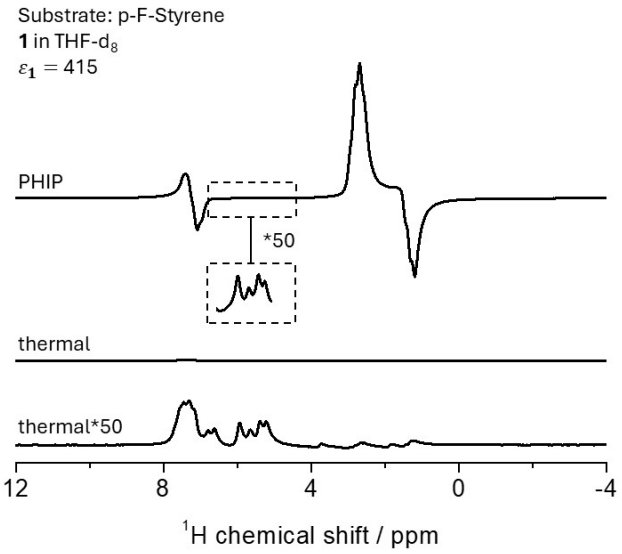

Figure S39. ^{1}H NMR spectra recorded during the hydrogenation of p-F-styrene in THF-d_8 catalysed by **1**: (top) ^{1}H PHIP spectrum after the addition of pH_2, (middle) thermal spectrum after 44 s, and (bottom) 50-times enlarged thermal spectrum. The spectra are normalized to the solvent peak at 3.6 ppm.

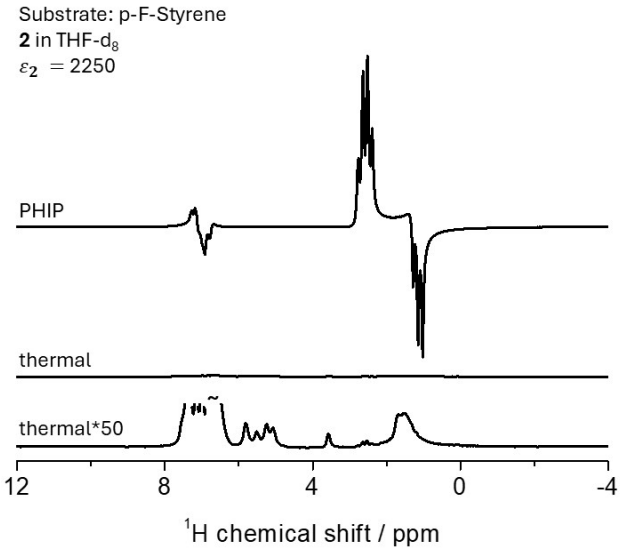

Figure S40. ^{1}H NMR spectra recorded during the hydrogenation of p-F-styrene in THF-d_8 catalysed by **2**: (top) ^{1}H PHIP spectrum after the addition of pH_2, (middle) thermal spectrum after 33 s, and (bottom) 50-times enlarged thermal. The spectra are normalized to the solvent peak at 3.6 ppm.

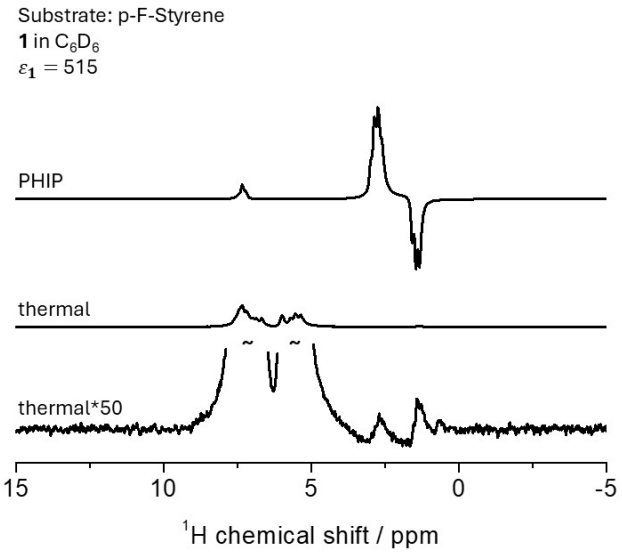

Figure S41. ^{1}H NMR spectra recorded during the hydrogenation of p-F-styrene in C_6D_6 catalysed by **1**: (top) 1H PHIP spectrum after the addition of pH_2, (middle) thermal spectrum after 22 s, and (bottom) 50-times enlarged thermal spectrum. The spectra are normalized to the solvent peak at 7.2 ppm.

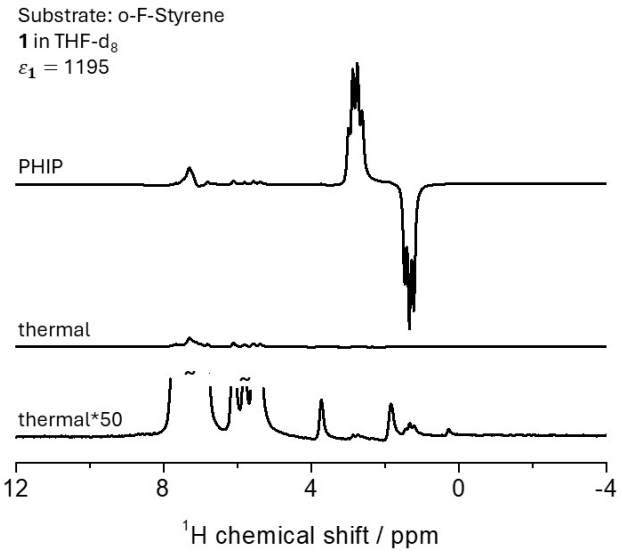

Figure S42. ^{1}H NMR spectra recorded during the hydrogenation of o-F-styrene in THF-d_8 catalysed by **1**: (top) ^{1}H PHIP spectrum after the addition of pH_2, (middle) thermal spectrum after 14 s, and (bottom) 50-times enlarged thermal spectrum. The spectra are normalized to the solvent peak at 3.6 ppm.

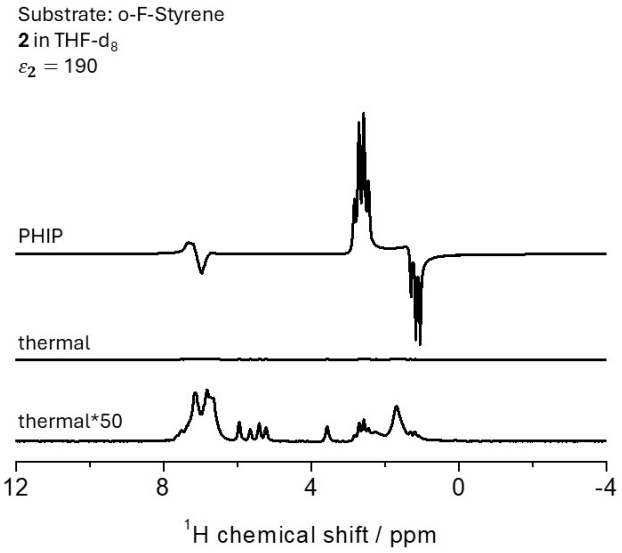

Figure S43. ^{1}H NMR spectra recorded for the hydrogenation of o-F-styrene in THF-d_8 catalysed by **2**: (top) ^{1}H PHIP spectrum after the addition of pH_2, (middle) thermal spectrum after 23 s, and (bottom) 50-times enlarged thermal spectrum. The spectra are normalized to the solvent peak at 3.6 ppm.

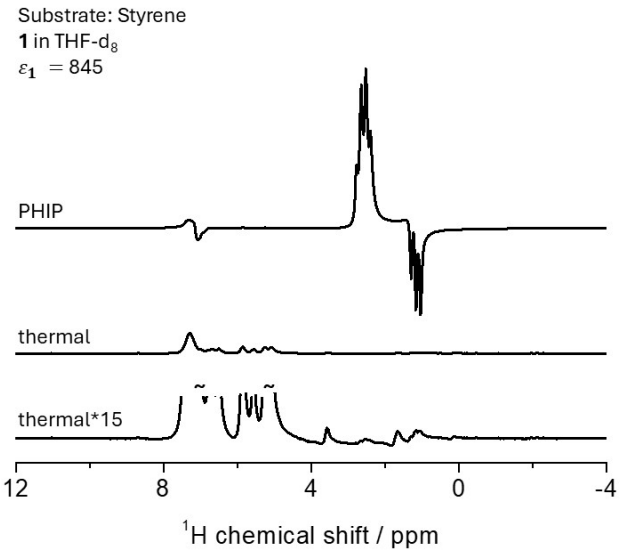

Figure S44. ^{1}H NMR spectra recorded during the hydrogenation of styrene in THF-d_8 catalysed by **1**: (top) ^{1}H PHIP spectrum after the addition of pH_2, (middle) thermal spectrum after 60 s, and (bottom) 15-times enlarged thermal spectrum. The spectra are normalized to the solvent peak at 3.6 ppm.

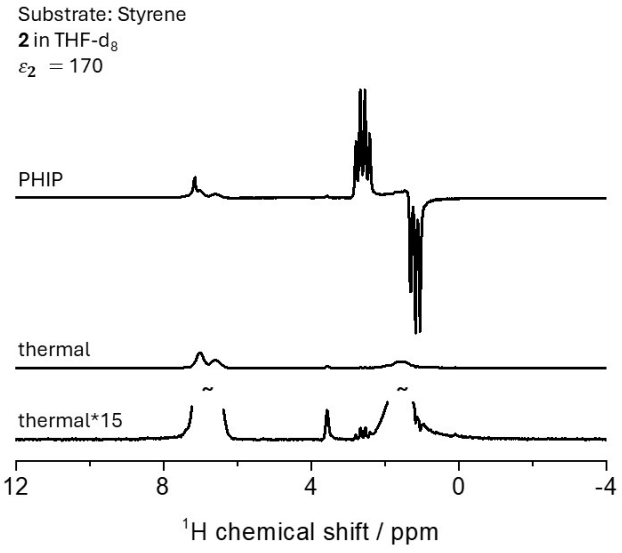

Figure S45. ^{1}H NMR spectra recorded during the hydrogenation of styrene in THF-d_8 catalysed by **2**: (top) ^{1}H PHIP spectrum after the addition of pH_2, (middle) thermal spectrum after 17 s, and (bottom) 15-times enlarged thermal spectrum. The spectra are normalized to the solvent peak at 3.6 ppm.

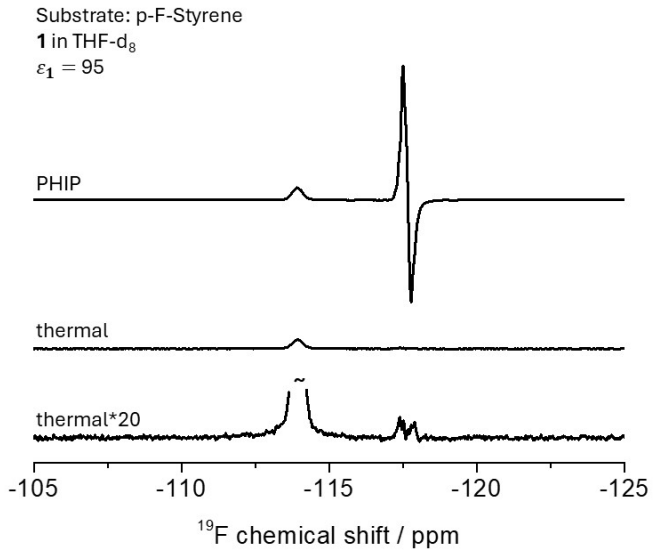

Figure S46. ^{19}F NMR spectra recorded during the hydrogenation of p-F-styrene in THF-d_8 catalysed by **1**: (top) ^{19}F PHIP spectrum after the addition of pH_2, (middle) thermal spectrum after 19 s, and (bottom) 20-times enlarged thermal spectrum.

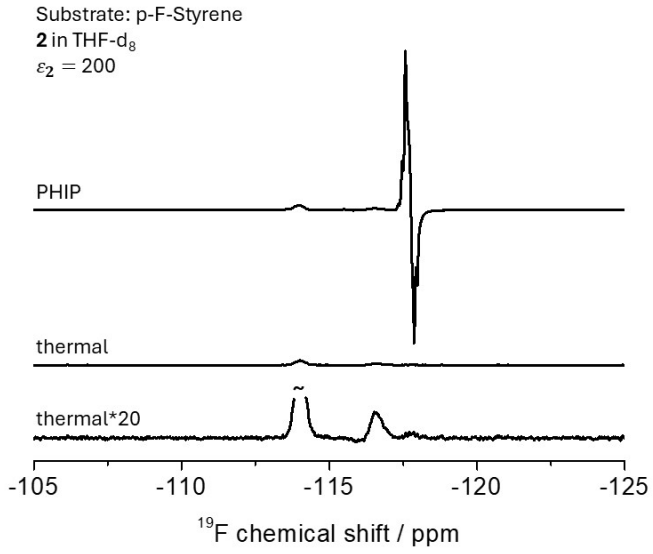

Figure S47. ^{19}F NMR spectra recorded during the hydrogenation of p-F-styrene in THF-d_8 catalysed by **2**: (top) ^{19}F PHIP spectrum after the addition of pH_2, (middle) thermal spectrum after 45 s, and (bottom) 20-times enlarged thermal spectrum.

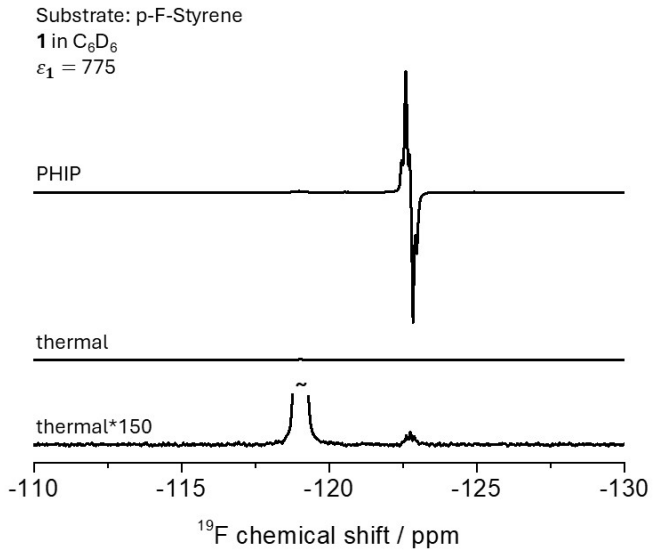

Figure S48. ^{19}F NMR spectra recorded during the hydrogenation of p-F-styrene in C_6D_6 catalysed by **2**: (top) ^{19}F PHIP spectrum after the addition of pH_2, (middle) thermal spectrum after 27 s, and (bottom) 150-times enlarged thermal spectrum.

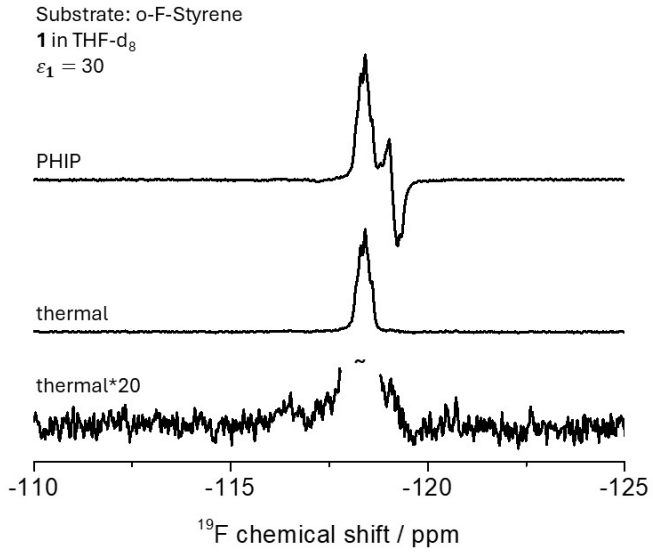

Figure S49. ^{19}F NMR spectra recorded during the hydrogenation of o-F-styrene in THF-d_8 catalysed by **1**: (top) ^{19}F PHIP spectrum after the addition of pH_2, (middle) thermal spectrum after 9 s, and (bottom) 20-times enlarged thermal spectrum.

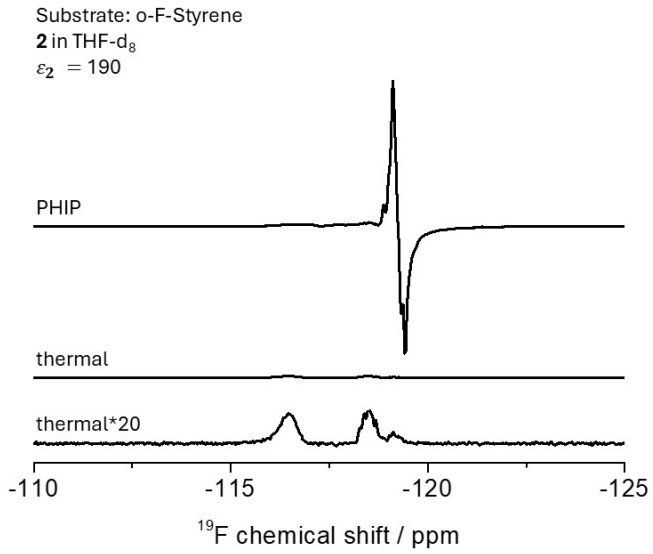

Figure S50. ^{19}F NMR spectra recorded during the hydrogenation of o-F-styrene in THF-d_8 catalysed by **2**: (top) ^{19}F PHIP spectrum after the addition of pH_2, (middle) thermal spectrum after 32 s, and (bottom) 20-times enlarged thermal spectrum.

3 Electronic structure of 1 and 2

3.1 Summary of electronic structure data for 1 and 2

We have previously investigated the electronic structure of **1** and **2** using Mößbauer spectroscopy (for **1**) and Broken-Symmetry DFT calculation to account for the ligand non-innocence. These data are summarised below and were previously reported in reference 1 and 18.

Complex 1:

Table S2. Optimization results of **1** for various spin states. Level of theory: optimization B3LYP, SVP//TZVP(-f), Mößbauer: B3LYP/def2-TZVP//CP(PPP) for Fe. L = PNN ligand.

				Mößbauer[b]	
Input	Converged to	$S_{\alpha\beta}$	ΔG^a	δ	$\lvert\Delta E_Q\rvert$
experimental	-	-	-	0.40	1.05
RKS	RKS	-	12.4	0.31	1.26
^{1}UKS (S = 0)	BS(1,1,1,1) L^{up}-Fe^{down}-Fe^{down}-L^{up}	0.53/0.48	0.4	0.43	1.25
BS(1,1)	BS(1,1,1,1) L^{up}-Fe^{down}-Fe^{up}-L^{down}	0.52/0.49	0.0	–	–
BS(2,2)	BS(1,1,1,1) L^{down}-Fe^{up}-Fe^{up}-L^{down}	0.53/0.48	–	–	–
^{3}UKS	L^{down}-Fe^{up}-Fe^{up}-L^{up}	0.51/0/0	3.7	–	–

a – in kcal/mol; *b* – in mm/s

Consequently, the compound is best described as a ls-Fe(I) species, antiferromagnetically coupled with a ligand radical, giving rise to an open-shell singlet ground state (S = 0). The first excited state (triplet) is 3.7 kcal/mol higher in energy.

Complex 2:

Table S3. Solutions for the ground state electronic structure of **2** obtained from DFT calculations.[1]
Level of theory: optimization: B3LYP, TZVP, CPCM(THF), Mößbauer: B3LYP/def2-TZVP//CP(PPP) for Fe. L = PNN ligand.

				Mößbauer[b]	
Input	Converged to	$S_{\alpha\beta}$	ΔG^a	δ	$\lvert\Delta E_Q\rvert$
experimental	-	-	-	0.12	1.06
RKS	-	-	1.3	0.08	1.23
^{1}UKS (S = 0)	RKS	1.0/1.0	0.9	-	-
BS(1,1)	RKS	1.0/1.0	0.0	0.08	1.23
^{3}UKS	triplet: Fe^{up}-L^{up}	0/0	9.2	-	-

a – in kcal/mol; *b* – in mm/s

The calculation of the Mößbauer parameters was performed as described in reference 18 and its supporting information. A singlet ground state is in line with NMR spectroscopy, which suggests **2** is a diamagnetic compound. This was further corroborated by DFT calculations. In contrast to **1** (**Table S2**), all Broken Symmetry approaches have converged to a closed-shell singlet solution, while a triplet ground state is 9.2 kcal/mol higher in energy.[1]

To further corroborate this formulation with experimental data, we have recorded the Mößbauer spectrum of **2** (see **Figure S52**). The experimental isomer shift and quadrupole splitting agree with the calculated values based on the closed-shell singlet solution.

Based on the bond lengths and NMR chemical shifts, compound **2** can be formulated both as a Fe(0) centre, stabilised by a neutral PNN chelate, or a Fe(II) centre, stabilised by a dianionic PNN chelate, based on a dearomatized pyridine core. The current spectroscopic data do not allow us to differentiate between these two forms. The results are summarised in **Figure S51**, below.

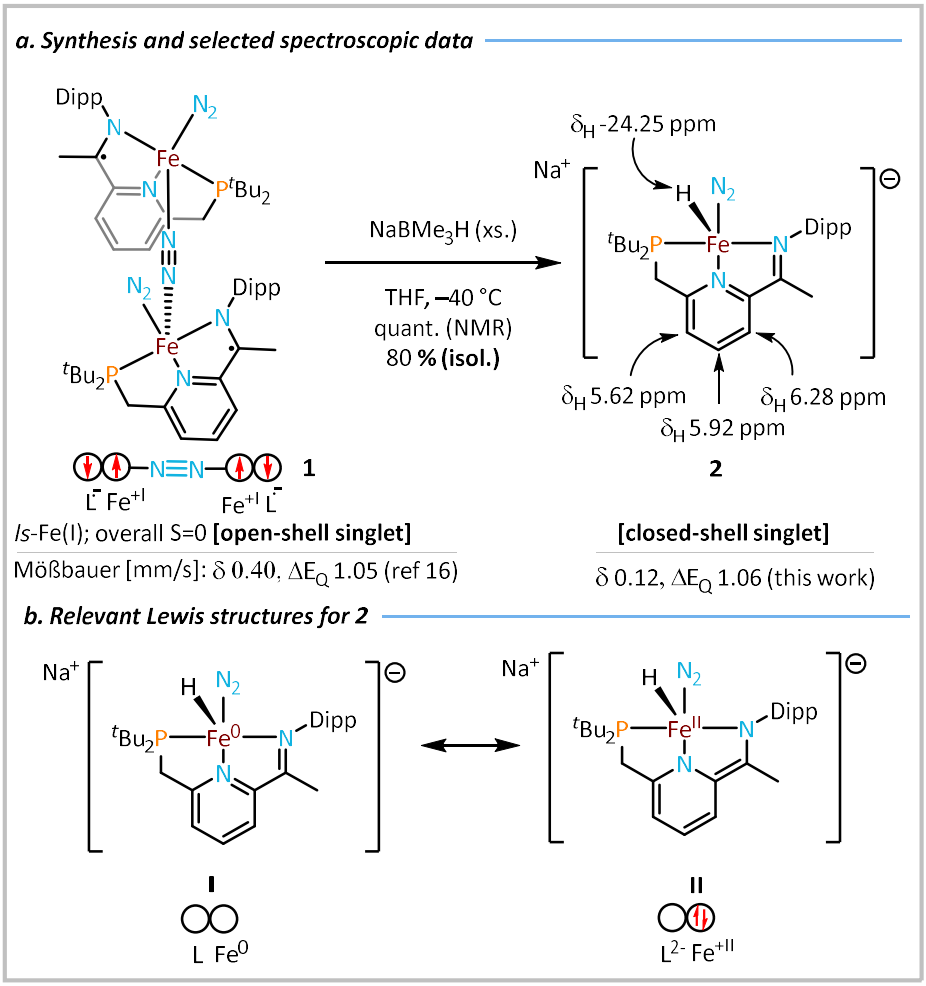

Figure S51. Synthesis, spectroscopic data, electronic- and Lewis structures of complexes **1** and **2**.

3.2 Experimental details for Mößbauer spectroscopy

^{57}Fe Mößbauer data were recorded on spectrometers with alternating constant acceleration in Mülheim/Ruhr (Max-Planck-Institut für Chemische Energiekoversion). The minimum experimental line width was 0.24 mm/s (full width at half-height) and the source was ^{57}Co/Rh. The sample temperature was maintained constant either in an Oxford Instruments Variox cryostat or in a Wissel MBBC-HE0106 bath cryostat. Isomer shifts are quoted relative to iron metal at room temperature. Simulations were performed with the JulX Software developed by Dr. Eckhard Bill at the Max-Planck-Institut für Chemische Energiekonversion.

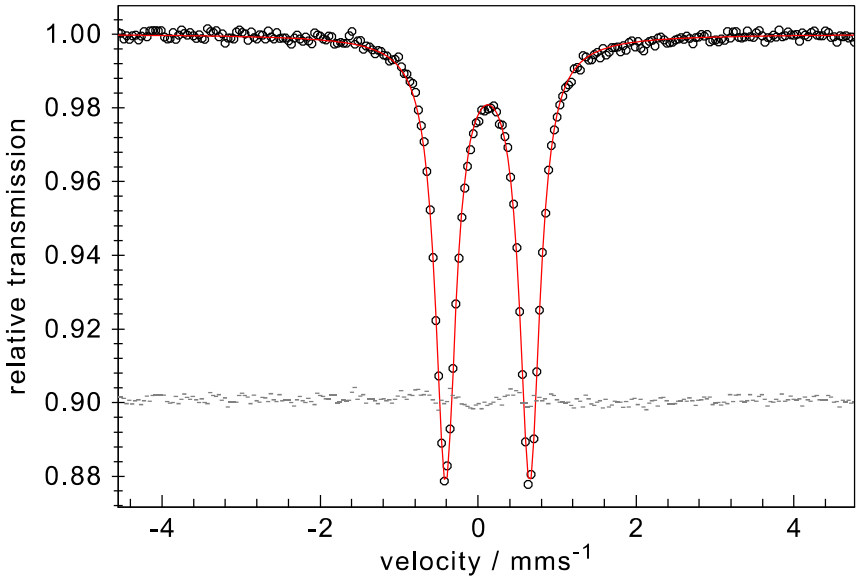

Figure S52. Zero-field ^{57}Fe-Mößbauer spectrum (80 K) of **2**. The fit of the data with a Lorentzian doublet yielded the following values: δ = 0.12 mm·s^{-1} and $|\Delta E_Q|$ = 1.06 mm·s^{-1}.

4 References

1 N. I. Regenauer, H. Wadepohl, D.-A. Roşca, *Inorg. Chem.*, 2022, **61**, 7426-7435.

2 G. Dilauro, A. Francesca Quivelli, P. Vitale, V. Capriati, F. M. Perna, *Angew. Chem. Int. Ed.*, 2019, **58**, 1799-1802.

3 N. G. Léonard, P. J. Chirik, *ACS Catalysis*, 2018, **8**, 342-348.

4 M. C. Haibach, B. M. Stoltz, R. H. Grubbs, *Angew. Chem. Int. Ed*., 2017, **56**, 15123-15126.

5 Z.Yu, Y. Lv, C. Yu, W. Su, *Tetrahedron Letters*, 2013, **10**, 1261-1263.

6 T. Bai, T. James, D. Song, *Dalton Trans.*, 2017, **46**, 12408-12412.

7 J. J. Dunsford, E. R. Clark, M. J. Ingleson, *Angew. Chem. Int. Ed.*, 2015, **54**, 5688-5692.

8 Y. Sunada, H. Tsutsumi, K. Shigeta, R. Yoshida, T. Hashimoto, H. Nagashima, *Dalton Trans.*, 2013, **42**, 16687-16692.

9 D. C. Najera, M. N. Peñas-Defrutos, M. García-Melchor, A. R. Fout, *Inorg. Chem.*, 2024, **63**, 17706-17713.

10 K. T. Neumann, S. Klimczyk, M. N. Burhardt, B. Bang-Andersen, T. Skrydstrup, A. T. Lindhardt, *ACS Catalysis*, 2016, **6**, 4710-4714.

11 M. Espinal-Viguri, S. E. Neale, N. T. Coles, S. A. Macgregor, R. L. Webster, *J. Am. Chem. Soc.*, 2019, **141**, 572-582.

12 S. J. Alavi, H. Sadeghian, S. M. Seyedi, H. Eshghi, A. Salimi, *Appl Organometal Chem*., 2018, **32**, e4167.

13 S. C. Bart, E. Lobkovsky and P. J. Chirik, *J. Am. Chem. Soc.*, 2004, **126**, 13794-13807.

14 J. Eills, D. Budker, S. Cavagnero, E. Y. Chekmenev, S. J. Elliott, S. Jannin, A. Lesage, J. Matysik, T. Meersmann, T. Prisner, J. A. Reimer, H. Yang, I. V. Koptyug, *Chem. Rev.*, 2023, **123**, 1417–1551.

15 M. G. Pravica, D. P. Weitekamp, *Chem. Phys. Lett.*, 1988, **145**, 255–258.

16 D. A. Barskiy, A. M. Coffey, P. Nikolaou, D. M. Mikhaylov, B. M. Goodson, R. T. Branca, G. J. Lu, M. G. Shapiro, V.-V. Telkki, V. V. Zhivonitko, I. V. Koptyug, O. G. Salnikov, K. V. Kovtunov, V. I. Bukhtiyarov, M. S. Rosen, M. J. Barlow, S. Safavi, I. P. Hall, L. Schröder, E. Y. Chekmenev*, Chem. Eur. J.,* 2017, **23**, 725–751.

17 D. C. Najera and A. R. Fout, *J. Am. Chem. Soc.*, 2023, **145**, 21086-21095.

18 N. I. Regenauer, H. Wadepohl, D.-A. Roşca, *Chem. Eur. J.*, 2022, e202202172.